

1 **Colony formation in *Phaeocystis antarctica*: connecting molecular**
2 **mechanisms with iron biogeochemistry**

3 Sara J. Bender^{a,b}, Dawn M. Moran^a, Matthew R. McIlvin^a, Hong Zheng^c, John P. McCrow^c,
4 Jonathan Badger^{c,f}, Giacomo R. DiTullio^c, Andrew E. Allen^{c,d}, Mak A. Saito^{a,*}

5 ^aMarine Chemistry and Geochemistry Department, Woods Hole Oceanographic Institution,
6 Woods Hole, Massachusetts 02543 USA

7 ^bCurrent address: Gordon and Betty Moore Foundation, Palo Alto, California 94304 USA

8 ^cMicrobial and Environmental Genomics, J. Craig Venter Institute, La Jolla, California 92037
9 USA

10 ^dIntegrative Oceanography Division, Scripps Institution of Oceanography, UC San Diego, La
11 Jolla, California 92037 USA

12 ^eCollege of Charleston, Charleston South Carolina 29412, USA

13 ^fCurrent address: Center for Cancer Research, Bethesda, Maryland 20892, USA

14 *Correspondence to M. Saito (msaito@whoi.edu)

15

16

17 *In Minor Revision at Biogeosciences*

18 *July 20, 2018*

19 *Submitted version*

20 **Abstract.**

21 *Phaeocystis antarctica* is an important phytoplankter of the Ross Sea where it dominates the early
22 season bloom after sea ice retreat and is a major contributor to carbon export. The factors that
23 influence *Phaeocystis* colony formation and the resultant Ross Sea bloom initiation have been of
24 great scientific interest, yet there is little known about the underlying mechanisms responsible for
25 these phenomena. Here, we present laboratory and field studies on *Phaeocystis antarctica* grown
26 under multiple iron conditions using a coupled proteomic and transcriptomic approach. *P.*
27 *antarctica* had a lower iron limitation threshold than a Ross Sea diatom *Chaetoceros* sp., and at
28 increased iron nutrition (>120 pM Fe') a shift from flagellate cells to a majority of colonial cells
29 in *P. antarctica* was observed, implying a role for iron as a trigger for colony formation. Proteome
30 analysis revealed an extensive and coordinated shift in proteome structure linked to iron
31 availability and life cycle transitions with 327 and 436 of proteins measured were significantly
32 different between low and high iron in strains 1871 and 1374, respectively. The enzymes
33 flavodoxin and plastocyanin that can functionally replace iron metalloenzymes were observed at
34 low iron treatments consistent with cellular iron sparing strategies, with plastocyanin having a
35 larger dynamic range. The numerous isoforms of the putative iron-starvation induced protein ISIP
36 group (ISIP2A and ISIP3) had abundance patterns coincided with that of either low or high iron
37 (and coincident flagellate or the colonial cell types in strain 1871), implying that there may be
38 specific iron acquisition systems for each life cycle type. The proteome analysis also revealed
39 numerous structural proteins associated with each cell type: within flagellate cells actin and tubulin
40 from flagella and haptonema structures as well as a suite of calcium-binding proteins with EF
41 domains were observed. In the colony-dominated samples a variety of structural proteins were
42 observed that are also often found in multicellular organisms including spondins, lectins, fibrillins,

43 and glycoproteins with von Willebrand domains. A large number of proteins of unknown function
44 were identified that became abundant at either high and low iron availability. These results were
45 compared to the first metaproteomic analysis of a Ross Sea *Phaeocystis* bloom to connect the
46 mechanistic information to the *in situ* ecology and biogeochemistry. Proteins associated with both
47 flagellate and colonial cells were observed in the bloom sample consistent with the need for both
48 cell types within a growing bloom. Bacterial iron storage and B₁₂ biosynthesis proteins were also
49 observed consistent with chemical synergies within the colony microbiome to cope with the
50 biogeochemical conditions. Together these responses reveal a complex, highly coordinated effort
51 by *P. antarctica* to regulate its phenotype at the molecular level in response to iron and provide a
52 window into the biology, ecology, and biogeochemistry of this group.

53

54 **1. Introduction**

55 The genus *Phaeocystis* is a cosmopolitan marine phytoplankton group that plays a key role in
56 global carbon and sulfur cycles (Hamm et al., 1999; Matrai et al., 1995; Rousseau et al., 2007;
57 Schoemann et al., 2005; Smith et al., 1991; Solomon et al., 2003; Thingstad and Billen, 1994;
58 Verity et al., 2007). Because of their large cell concentrations during bloom formation, *Phaeocystis*
59 have a significant impact on the ocean biogeochemistry through carbon fixation (Arrigo et al.,
60 1999; Hamm et al., 1999; Matrai et al., 1995; Rousseau et al., 2007; Schoemann et al., 2005; Smith
61 et al., 1991; Solomon et al., 2003; Thingstad and Billen, 1994; Verity et al., 2007), the release of
62 large concentrations of organic carbon upon grazing/viral lysis (Alderkamp et al., 2007; Hamm et
63 al., 1999; Lagerheim, 1896; Verity et al., 2007), and export as aggregates out of the photic zone
64 (DiTullio et al., 2000). Through the production of dimethylsulfide (DMS), they also directly
65 connect ocean and atmospheric processes and carbon and sulfur cycling (Smith et al., 2003).

66 Some *Phaeocystis* species, including *Phaeocystis antarctica*, undergo multiple
67 morphotypes and can occur as flagellated single-cells or in gelatinous colonies consisting of
68 thousands of non-motile cells (Fig. 1). Microscopic and chemical analyses have found that
69 *Phaeocystis* colonies are filled with a mucilaginous matrix surrounded by a thin, but strong,
70 hydrophobic skin (Hamm, 2000; Hamm et al., 1999). Once formed, cells typically associate with
71 this outer layer of the colony (Smith et al., 2003). Colony formation involves the exudation of
72 (muco)polysaccharides and carbohydrate-rich dissolved organic matter, as well as amino sugars
73 and amino acids; it is estimated that approximately 50 – 80% of *Phaeocystis* carbon is allocated to
74 this extracellular matrix (Hamm et al., 1999; Matrai et al., 1995; Rousseau et al., 2007; Solomon
75 et al., 2003; Thingstad and Billen, 1994). Thus, not only does the colony increase the size of
76 *Phaeocystis* by several orders of magnitude, but the extracellular matrix material also constitutes
77 the majority of measured algal (carbon) biomass (Rousseau et al., 1990). The colonial form of
78 *Phaeocystis* has been suggested as a defense mechanism against grazers (Hamm et al., 1999), a
79 means to sequester micronutrients such as iron and manganese (Noble et al., 2013; Schoemann et
80 al., 2001), as a means of protection from pathogens (Hamm, 2000; Jacobsen et al., 2007), and as a
81 microbiome vitamin B₁₂ source (Bertrand et al., 2007). Colony formation of *Phaeocystis* species,
82 including *P. antarctica* and *P. globosa*, has been linked to numerous physiological triggers
83 including the synergistic effects of iron and irradiance (Feng et al., 2010), grazer-induced chemical
84 cues (Long et al., 2007), phosphate concentrations (Riegman et al., 1992), and the presence of
85 different nitrogen species (Riegman and van Boekel, 1996; Smith et al., 2003).

86 The Ross Sea is one of the most productive regions of the Southern Ocean (Arrigo et al.,
87 1999; 1998; Feng et al., 2010; Garcia et al., 2009; Sedwick and DiTullio, 1997), and the latter is
88 an important contributor to the cycling of carbon in the oceans (Lovenduski et al., 2008; Sarmiento

89 et al., 1998). In the early spring when the sea ice retreats and polynyas form, phytoplankton blooms
90 and regional phytoplankton productivity are fed by the residual winter iron inventory and perhaps
91 iron-rich sea ice melt (Noble et al., 2013; Sedwick and DiTullio, 1997); blooms have also been
92 linked to changes in irradiance and mixed layer depth (Arrigo et al., 1999; Coale et al., 2003;
93 Martin et al., 1990; Sedwick and DiTullio, 1997; Sedwick et al., 2000). In the Ross Sea Polynya
94 (RSP), *P. antarctica* colonial cells form almost mono-specific blooms until the austral
95 summer season begins, comprising > 98% of cell abundance at the peak of the bloom (Smith et
96 al., 2003). Although diatom abundance dominates in the summer, the RSP typically harbors
97 the co-existence of flagellated single cells of *P. antarctica* along with diatoms (Garrison et al.,
98 2003). During blooms *P. antarctica* can draw down more than twice as much carbon relative to
99 phosphate as diatoms and contribute to rapid carbon export, leaving a lasting biogeochemical
100 imprint on surrounding waters (Arrigo et al., 1999; 2000; DiTullio et al., 2000; Dunbar et al.,
101 1998). Recent *in vitro* iron addition experiments provide evidence that iron nutrition influences *P.*
102 *antarctica* growth in this region, with increasing *P. antarctica* biomass in incubation experiments
103 (Bertrand et al., 2007; Feng et al., 2010). Moreover, laboratory experiments with *P. antarctica*
104 have observed a high cellular iron requirement and variable use of strong organic iron complexes
105 (Sedwick et al., 2007; Strzepek et al., 2011; Luxem et al., 2017).

106 The multiphasic lifecycle of *P. antarctica* in the Ross Sea gives it a spectrum of nutrient
107 drawdown phenotypes and trophic interactions, dependent on the presence of flagellated versus
108 colonial cells (Smith et al., 2003). Given its prominence during early spring sea ice retreat, it has
109 been hypothesized that the triggers of colony formation for *Phaeocystis* cells are also the triggers
110 of the spring phytoplankton bloom. Yet experimental and molecular analyses of potential
111 environmental triggers and how they manifest in changes in cellular morphology have remained

112 elusive. Little is known about the mechanisms responsible for colony formation in *P. antarctica*,
113 nor how these mechanisms respond to an environmental stimulus such as iron, both of which
114 appear to be integral to the ecology and biogeochemistry of *P. antarctica*.

115 **2. Materials and methods**

116 **2.1 Culture experiments**

117 Two strains of *Phaeocystis antarctica* (treated with Provasoli's antibiotics), CCMP 1871 and
118 CCMP 1374 (Provasoli-Guillard National Center for Culture of Marine Phytoplankton), and a
119 Ross Sea centric diatom isolate *Chaetoceros* sp. RS-19 (collected by M. Dennett at 76.5° S, 177.1°
120 W in December 1997 and isolated by D. Moran) were grown in F/2 media with a trace metal stock
121 (minus FeCl₃) according to Sunda and Huntsman (Sunda and Huntsman, 2003; 1995), using a
122 modified 10 μM EDTA concentration, and an oligotrophic seawater base. Strains were chosen
123 because they were culturable representatives from two distinct regions in the Southern Ocean.

124 Semi-continuous batch cultures were grown at 4 °C under 200 μmol photons m⁻² s⁻¹
125 continuous light. Each strain was acclimated to growth on one of six growth condition
126 concentrations: the concentration of dissolved inorganic iron within each treatment was 2 pM, 41
127 pM, 120 pM, 740 pM, 1200 pM, and 3900 pM Fe' as set by the metal buffer EDTA (where
128 Fe'/Fe_{Total} = 0.039) (Sunda and Huntsman, 2003). During the experiment, cultures were maintained
129 in 250 mL polycarbonate bottles; and, subsamples were collected every 1-2 days in 5 mL 13x100
130 mm borosilicate tubes to measure relative fluorescence units (RFUs) and cell counts in the
131 treatments. Mid-to-late exponential phase cultures were harvested for transcriptome and proteome
132 analysis and cell size was measured for both strains; cell pellets were stored at -80 °C (see
133 Supplementary Information for additional methods). Cell counts were conducted using a Palmer-
134 Maloney counting chamber and a Zeiss Axio Plan microscope on 400x magnification; cell

135 numbers were used to determine the final growth rate of each strain/treatment. During mid-to-late
136 exponential phase (time-of-harvest), cell size was determined for both strains (n=20 cells were
137 counted for each strain), calculated using the Zeiss 4.8.2 software and a calibrated scale bar. The
138 number of cells in colonies (versus as single cells) was determined for strain 1871 only. Briefly,
139 counts (number of cells associated with colonies versus unassociated) were averaged from 10
140 fields of view at five distinct time points (50 fields of view total).

141

142 **2.2 Protein extraction, digestion, and mass spectrometry analyses**

143 Proteins from cell pellets (one pellet per treatment, two strains and six iron treatments for a total
144 of 12 proteomes) was extracted using the detergent B-PER (Thermo Scientific), quantified,
145 purified by immobilization within an acrylamide tube gel, trypsin digested, alkylated and reduced,
146 and analyzed by liquid chromatography-mass spectrometry (LC-MS) using a Michrom Advance
147 HPLC with a reverse phase C18 column (0.3 x 10 mm ID, 3 μm particle size, 200 \AA pore size,
148 SGE Protocol C18G; flow rate of 1 $\mu\text{L min}^{-1}$, nonlinear 210 min gradient from 5% to 95% buffer
149 B, where A was 0.1% formic acid in water and B was 0.1% formic acid in acetonitrile, all solvents
150 were Fisher Optima grade) coupled to a Thermo Scientific Q-Exactive Orbitrap mass spectrometer
151 with a Michrom Advance CaptiveSpray source. The mass spectrometer was set to perform MS/MS
152 on the top 15 ions using data-dependent settings (dynamic exclusion 30 s, excluding unassigned
153 and singly charged ions), and ions were monitored over a range of 380-2000 m/z (see
154 Supplementary Information for detailed protocol). Peptide-to-spectrum matching was conducted
155 using the SEQUEST algorithm within Proteome Discoverer 1.4 (Thermo Scientific) using the
156 translated transcriptomes for *P. antarctica* strain 1871 and strain 1374 (Fig 2., see below).
157 Normalized spectral counts were generated from Scaffold 4.0 (Proteome Software Inc.), with a

158 protein false discovery rate (FDR) of 1.0%, a minimum peptide score of 2, and a peptide
159 probability threshold of 95%. Spectral counts refer to the number of peptide-to-spectrum matches
160 that are attributed to each predicted protein from the transcriptome analysis, and the Scaffold
161 normalization scheme involves a small correction normalizing the total number of spectra counts
162 across all samples to correct for run-to-run variability and improve comparisons between
163 treatments. The R package “FactoMineR” (Lê et al., 2008) was used for the PCA analysis; for
164 heatmaps, the package “gplots” was used (Warnes et al., 2009). Proteomic samples taken from
165 each laboratory condition were not pooled downstream as part of the analyses; replicates shown
166 for each treatment are technical replicates.

167

168 **2.3 RNA extraction, Illumina sequencing, and annotation**

169 For *P. antarctica* cultures total RNA was isolated from cell pellets (one pellet per treatment, two
170 strains and three iron concentrations for a total of six transcriptomes) following the TRIzol Reagent
171 (Life Technologies, manufacturer’s protocol). RNeasy Mini kit (Qiagen) was used for RNA
172 cleanup, and DNase I (Qiagen) treatment was applied to remove genomic DNA. Libraries, from
173 polyA enrichment mRNA, were constructed using a TruSeq RNA Sample Preparation Kit V2
174 (Illumina™), following the manufacturer’s TruSeq RNA Sample Preparation Guide. Sequencing
175 was performed using the Illumina HiSeq platform. Downstream, reads were trimmed for quality
176 and filtered. CLC Assembly Cell (CLCbio) was used to assemble contigs, open reading frames
177 (ORFs) were predicted from the assembled contigs using FragGeneScan (Rho et al., 2010), and
178 additional rRNA sequences were removed. The remaining ORFs were annotated de novo via
179 KEGG, KO, KOG, Pfam, and TigrFam assignments. Taxonomic classification was assigned to
180 each ORF and the Lineage Probability Index (LPI, as calculated in (Podell and Gaasterland, 2007)).

181 ORFs classified as Haptophytes were retained for downstream analyses. Analysis of sequence
182 counts (“ASC”) was used to assign normalized fold change and determine which ORFs were
183 significantly differentially expressed in pairwise comparisons between treatments. The ASC
184 approach offers a robust analysis of differential gene expression data for non-replicated samples
185 (Wu et al., 2010).

186 For metatranscriptomes, RNA was extracted from frozen cell pellets using the TRIzol
187 reagent manufacturer’s protocol (Thermo Fisher Scientific) (see Supplementary Information for
188 additional details on metatranscriptome processing).

189

190 **2.4 Ross Sea *Phaeocystis* bloom: sample collection and protein extraction and analysis**

191 The meta ’omics samples were collected in the Ross Sea (170.76° E, 76.82° S) during the
192 CORSACS expedition (Controls on Ross Sea Algal Community Structure) on December 30, 2005
193 (near pigment station 137; <http://www.bco-dmo.org/dataset-deployment/453377>) (Saito et al.,
194 2010; Sedwick et al., 2011). Surface water was concentrated via a plankton net tow (20 µm mesh),
195 gently decanted of extra seawater, then split into multiple replicate cryovials and frozen in
196 RNAlater at -80 °C for metatranscriptome and metaproteome analysis. The pore size of the net
197 tow would have preferentially captured the colony form of *Phaeocystis*, although filtration with
198 small pore size membrane filters was particularly challenging during this time period due to the
199 abundance of *Phaeocystis* colonies and the clogging effect of their mucilage. Moreover, the
200 physical process of deploying the net tow appears to have entrained some smaller cells including
201 the *Phaeocystis* flagellate cells by adsorption to partially broken colonies and associated mucilage
202 as observed in the metaproteome results. Two of these replicate bloom samples were frozen for

203 proteome analysis. A third replicate sample from this field site was extracted for
204 metatranscriptome analysis as described above.

205 Proteins were extracted, digested, and purified following the lab methods above, and then
206 identified first on a Thermo Q-Exactive Orbitrap mass spectrometer using a Michrom Advance
207 CaptiveSpray source, then samples were subsequently re-run on a two-dimensional
208 chromatographic nanoflow system for increased metaproteomic depth on a Thermo Fusion
209 Orbitrap mass spectrometer (see supplemental materials for further details). Proteins were then
210 identified within the mass spectra using three databases (Fig. 2): the translated transcriptome
211 database for both *Phaeocystis* strains (Database #1), a Ross Sea metatranscriptome generated in
212 parallel from this metaproteome sample (Database #2; this transcriptome is a combination of
213 eukaryotic and prokaryotic communities derived from total RNA and poly(A) enriched RNA
214 sequencing), and a compilation of five bacterial metagenomes from the Amundsen Sea polynya
215 (Database #3) (Delmont et al., 2014), using SEQUEST within Proteome Discoverer 1.4 (Thermo
216 Scientific) (Eng et al., 1994) and collated with normalized spectral counts in Scaffold 4.0
217 (Proteome Software Inc.) (see Supplementary Information for additional details).

218

219 **2.5 Data availability**

220 *Phaeocystis antarctica* RNA sequence data reported in this paper have been deposited in the NCBI
221 sequence read archive under BioProject accession no. PRJNA339150, BioSample accession nos.
222 SAMN05580299 – SAMN05580303. Ross Sea metatranscriptomes have been deposited under
223 BioProject accession no. PRJNA339151, BioSample accession nos. SAMN05580312 –
224 SAMN05580313. Proteomic data from the lab and field components was submitted to the Pride
225 database (Project Name: *Phaeocystis antarctica* CCMP 1871 and CCMP 1374, Ross Sea

226 *Phaeocystis* bloom, LC-MSMS; Project accession: PXD005341; Project DOI:
227 10.6019/PXD005341).

228

229 **3. Results and discussion**

230 **3.1 Physiological response to iron availability: Growth limitation and colony formation**

231 The two strains of *P. antarctica* (1374 and 1871 hereon) were acclimated to six iron concentrations
232 to capture the metabolic response under different iron regimes (Fig. 3*a* and *b*). A biphasic response
233 in *P. antarctica* strain 1871 was observed; cultures exhibited a clear single-cell versus colony
234 response to low and high iron, respectively, that were observed by microscopy and were readily
235 apparent by naked eye due to the millimeter size of the colonies. The three low iron treatments (2
236 pM, 41 pM, and 120 pM Fe³⁺) cultures contained only single, flagellated cells, whereas the three
237 higher iron treatments (740 pM, 1200 pM, and 3900 pM Fe³⁺) had a majority of colonial cells,
238 based on detailed microscopy counts shown in Fig. 3*c*. This influence of iron on colony abundance
239 was observed in an additional experiment, where colonial cells were again absent at the lowest
240 three iron concentrations and were present at the three higher concentrations (Fig. S10). The
241 presence of both colony and flagellate cells is expected in actively growing populations with
242 colonies since reproduction is thought to require revisiting the flagellate life cycle stage. Single
243 cells and colonies were not counted in experiments with strain 1374, as these experiments were
244 conducted prior to those of 1871 and the iron-induced colony formation observations therein.
245 However, strain 1374 was observed to become “clumpy” at high iron. This clumping observation
246 may reflect the loss of a specific factor needed for the colony completion lost during long-term
247 maintenance in culture. This interpretation is consistent with the overall similar structural protein
248 expression patterns observed in both strains described below. Strzepek et al. also observed co-

249 varying of iron concentration and colony formation in some strains of *P. antarctica* (Strzepek et
250 al., 2011).

251 The two strains of *P. antarctica* were able to maintain growth rates for all but the lowest
252 of iron concentrations used here, similar to prior studies of *P. antarctica* strain AA1 that observed
253 no effect of scarce iron on growth rates (Strzepek et al., 2011). Parallel experiments with polar
254 diatoms such as *Chaetoceros* (Fig. 3d) observed growth limitation at moderate iron abundances
255 using an identical media composition, indicating 1) that *P. antarctica* has an impressive capability
256 for tolerating low iron compared to *Chaetoceros* and other diatoms (e.g. a Ross Sea *Pseudo-*
257 *nitzschia* sp. isolate, data not shown), and 2) demonstrating an absence of iron contamination in
258 these experiments. Growth rates for 1871 were significantly different between the 2 pM Fe'
259 treatment and all other treatments (student's t-test with Bonferroni correction, $p < 0.05$; Fig. 3a);
260 there were no significant differences among growth rates for strain 1374 (Fig. 3b). Cell size
261 (including both flagellate and colonial cells) decreased with lower iron concentration, a trend that
262 was statistically significant (ANOVA with TukeyHSD test, $p < 0.05$) for both strains when cell
263 sizes from each high iron treatment (740 pM, 1200 pM, and 3900 pM Fe') were compared to cell
264 sizes from each low iron treatment (2 pM, 41 pM, and 120 pM Fe') (Fig. 3e and f).

265

266 **3.2 Molecular response to low and high iron concentrations**

267 Global proteomics enabled by peptide-to-spectra matching to transcriptome analyses,
268 revealed a clear statistically significant molecular transition across the iron gradient for each strain
269 (Fig. 4). The global proteome consisted of 536 proteins identified in strain 1871 and 1085 proteins
270 identified in strain 1374 (Table 1; Supplementary Data 1), after summing unique proteins across
271 the six iron treatments. There were 55 proteins identified in strain 1871 and 64 proteins in strain

272 1374 (Fig. 4) that drove the statistical separation of proteomes across iron treatments using
273 principle component analysis (PCA, Axis 1 PCA correlation coefficient ≥ 0.9 or ≤ -0.9). Axis one
274 accounted for 49% variance for 1871 and 36% variance for 1374. Moreover, using a Fisher Test
275 (P-value ≤ 0.05), 327 proteins (strain 1871) and 436 proteins (strain 1374) of those proteins
276 detected were identified as significantly different in relative protein abundance between
277 representative “low” (41 pM Fe’) and “high” (3900 pM Fe’) iron treatments. This significant
278 change in the proteome composition paralleled observations of a shift from flagellate to colonial
279 cells. Iron-starvation responses and iron metabolism were detected within the high and low iron
280 PCA protein subsets, including iron-starvation induced proteins (ISIPs), flavodoxin, and
281 plastocyanin, demonstrating a multi-faceted cellular response to iron scarcity (Fig. 5).
282 Surprisingly, there was also a highly pronounced signal in the proteome that appeared to reflect
283 the structural changes occurring in *P. antarctica*. These structural proteins included multiple
284 proteins with protein family (PFam) domains suggestive of extracellular function, adhesion, and/or
285 ligand binding, including putative glycoprotein domains (for example, spondin) that were present
286 in the high iron PCA subset in both strains (Fig. 5); the appearance of these proteins also
287 corresponded to the occurrence of colonies in strain 1871 (Fig. 1). Similarly, a distinct suite of
288 proteins was more abundant in the low iron PCA subset (Fig. 5), including proteins relating to cell
289 signaling (for example, calmodulin/EF-hand, PHD zinc ring finger). A number of proteins with
290 unknown function were also detected in the PCA subsets: 71% unknown for strain 1871 and 42%
291 unknown for strain 1374 of a total of 311 proteins annotated as hypothetical proteins
292 (Supplementary Dataset 1). Outside of the PCA analyses, additional iron and adhesion-related
293 proteins were identified that demonstrated a similar expression profile to the PCA subset
294 (Supplementary Fig. 1).

295 Identification and characterization of proteins and transcripts induced by iron scarcity are
296 valuable in improving an understanding of the adaptive biochemical function of these complex
297 phytoplankton as well as for their potential utility for development as environmental stress
298 biomarkers (Roche et al., 1996; Saito et al., 2014). The enzymes flavodoxin and plastocyanin,
299 which require no metal and copper, respectively and that functionally replace iron metalloenzymes
300 counterparts ferredoxin and cytochrome c6, had isoforms that increased in concentrations at the
301 lower iron treatments consistent with cellular iron sparing strategies (Fig. 6, Supplementary Fig.
302 2) (Peers and Price, 2006; Whitney et al., 2011; Zurbriggen et al., 2008). In strain 1374 however,
303 there was an increase in both of these iron-sparing systems at the highest iron concentration (Fig.
304 6d and 6f, Supplementary Table 1). While both experiments were in exponential growth at the
305 time of harvest, those of strain 1374 were as much as 7.6 fold denser in cell number than those of
306 strain 1874 (based on cell counts from treatments specifically used for transcriptome analyses),
307 and as a result the denser 1374 strain appears to have also experienced iron stress even at this
308 highest iron concentration as the high biomass depleted iron within the medium. Of these two iron
309 sparing enzymes, plastocyanin appeared to show a clearer increase in abundance at lower
310 environmental iron concentrations (Fig 6c and 6f). In contrast, some flavodoxin isoforms could be
311 interpreted as being constitutive, two of the three isoforms were still present in reasonable spectral
312 counts at higher iron concentrations (Figs. 6a and 6d). Prior measurements during a Ross Sea
313 colonial *P. antarctica* spring bloom in 1998 were consistent with this where ferredoxin
314 concentrations were below detection and flavodoxin present (Maucher and DiTullio, 2003). A
315 constitutive flavodoxin could help explain *P. antarctica*'s ability to tolerate all but the lowest iron
316 treatment observed in the physiological experiments (Fig 3a and 3b), and implies that the careful

317 selection of isoforms, or better, the inclusion of all isoforms of a protein biomarker of interest may
318 be valuable in interpreting complex field results.

319 There were also numerous isoforms of the iron-starvation induced proteins (ISIP) group
320 identified within the proteome of each *P. antarctica* strain: specifically 9 ISIP2A's and 3 ISIP3's
321 in strain 1871 and 3 ISIP2A's and 4 ISIP3's in strain 1374 (Supplementary Fig. 1; Supplementary
322 Table 1). These ISIPs were identified based on their transcriptome response to iron stress in
323 diatoms and most recently have been implicated in a diatom cell surface iron concentrating
324 mechanism (Allen et al., 2008; Morrissey et al., 2015). Interestingly in this *P. antarctica*
325 experiment, these ISIPs exhibited both “high” or “low” iron responses, where specific isoforms
326 were more abundant only under one of those respective conditions (Fig. 6). Given the
327 metamorphosis of *P. antarctica* between flagellate and colonial cell types observed by microscopy
328 and the proteome across the gradient in iron, we hypothesize that this diversity of iron stress
329 responses in the ISIP proteins may reflect the complexity associated with *P. antarctica*'s life cycle.
330 As the abundant winter iron and sloughed basal sea ice reserves are depleted, newly formed
331 colonial cells will inevitably find themselves in the iron-depleted environments that have been
332 characterized in the Ross Sea almost immediately upon bloom formation due to iron's small
333 dissolved inventory (Bertrand et al., 2015; Sedwick et al., 2011). As a result, *P. antarctica* may
334 have distinct iron stress protein isoforms associated specifically with the colonial cell type (such
335 as the high iron/colonial ISIP proteins, Figs. 5 and 6) in order to acquire scarce iron during blooms,
336 in addition to a distinct suite of iron stress proteins produced within the flagellate cells (low
337 iron/flagellate ISIP proteins, also Figs. 5 and 6). Given the rapid depletion of iron during Ross Sea
338 blooms, it is also conceivable that these iron acquisition proteins are constitutively expressed
339 within the colony morphotype, rather than being connected to an iron-sensing and regulatory

340 response system. Future short-term iron perturbation studies that would complement the steady-
341 state experiments presented here could further investigate this hypothesis. The multiplicity of ISIP
342 proteins produced within each strain also is consistent with the observation that both *P. antarctica*
343 strains maintained high growth rates even at the lower 41 and 120 pM Fe³⁺ concentrations,
344 compared to the diatom *Chaetoceros sp.* whose growth rate is less than 50% of maximal growth
345 in similar media (Fig. 3).

346

347 **3.3 Correspondence between RNA and protein biomolecules**

348 Many of the RNA transcripts of iron-related genes trended with their corresponding
349 proteins: 60% of the iron-related gene transcripts reflected the proteomic response in strain 1871,
350 whereas there was a 30% correspondence between iron-related transcripts and proteins in strain
351 1374 (Supplementary Fig. 1). In total, 47% of expressed proteins in strain 1871 and 26% of
352 proteins in strain 1374 shared expression patterns with associated transcripts (Fig. 7), consistent
353 with recent studies of proteome-transcriptome comparisons that showed limited coordination
354 between inventories of each type of biomolecule (Dyhrman, 2012). As mentioned above, while
355 both experiments were in exponential growth at the time of harvest, strain 1374 was 7.6 fold denser
356 in cell number than those of strain 1874 at that time. Hence, this decrease in transcript-proteome
357 coherence in strain 1374 may be related to harvesting in late-log growth phase, and reflects the
358 challenge of trying to conduct comparisons of these biomolecules that function on different cellular
359 timescales.

360 Examination of the transcriptome revealed a significant increase in transcripts for tonB-
361 like transporters, which can be associated with cross-membrane nutrient transport (e.g. for iron
362 siderophores complexes or vitamin B₁₂ (Bertrand et al., 2007; 2013; Morris et al., 2010) under high

363 iron for strain 1871; and, significantly greater transcript abundances for a putative flavodoxin for
364 strain 1374 under low iron consistent with its substitution for ferredoxin due to iron scarcity (Roche
365 et al., 1996).

366

367 **3.4 Observation of an iron-induced switch from single cells to colonies**

368 The strong connection of iron availability to putative structural components of *P.*
369 *antarctica* observed here served as an ideal opportunity to examine the genes and proteins involved
370 in morphological and life cycle transitions and colony construction in this phytoplankter that can
371 otherwise be experimentally difficult to trigger in isolation. *Phaeocystis* colonies have captured
372 the interest of scientists for more than a century (Hamm et al., 1999), yet next to nothing is known
373 about the molecular basis of their construction. Colonies have been considered a collection of
374 loosely connected cells embedded within a gel matrix, and hence described as “balls of jelly” or
375 “bags of water” (Hamm et al., 1999; Lagerheim, 1896; Verity et al., 2007). Results here suggest
376 significant transformations in the cellular proteome that corresponded to solitary and colonial
377 morphological stages, for example, involving structural proteins and proteins known to be post-
378 translationally modified such as glycoproteins or those containing glycoprotein-binding motifs. To
379 our knowledge, such an extensive proteome remodeling has yet to be observed for another colonial
380 organism, nor with the influence of any other environmental stimuli in the genus *Phaeocystis*. As
381 a result the details of this response, while fascinating, are challenging to interpret due to their
382 novelty.

383 A putative spondin protein exhibited one of the largest responses between low and high
384 iron in both strains with a greater than 20-fold increase in relative protein abundance and
385 normalized 11-fold change in transcript abundance in strain 1871, and a greater than 9-fold

386 increase in relative protein abundance and 3-fold change in transcript abundance in strain 1374
387 (Fig. 5a and Supplementary Data 1). Spondin proteins are known to be glycosylated, and to be a
388 component of the extracellular matrix (ECM) environment, which may enable multicellularity in
389 metazoans through cell adhesion, and have been found to help coordinate nerve cell development
390 through adhesion and repulsion (Michel et al., 2010; Tzarfati-Majar et al., 2011). Despite this large
391 variation in protein abundance, the function of spondins in eukaryotic phytoplankton, including
392 *Phaeocystis* remains largely unknown. Given their responsiveness to iron availability and
393 associated enrichment in colony rich cultures, these proteins could potentially contribute to ECM-
394 related adhesion of cells, to each other or the colony skin, or even perhaps to the mucilage interior.

395 Additional glycoproteins that exhibited a strong iron response in both strains include those
396 containing von Willebrand factor domains (for example, protein families PF13519, PF00092), and
397 fibrillin and lectin (Fig. 5 and Supplementary Fig. 1). In biomineralizing organisms, such as corals,
398 glycoproteins with von Willebrand domains are hypothesized to play a role in the formation of the
399 extracellular organic matrix through adhesion (Drake et al., 2013; Hayward et al., 2011) laying the
400 scaffolding for calcification. Orthologs of the von Willebrand proteins that contain these domains
401 have also been characterized in humans and have protein-binding capabilities, which are important
402 for coagulation (Ewenstein, 1997). These dynamic von Willebrand proteins appear to contribute
403 to the cell aggregation and colony formation of *P. antarctica* colonies.

404 The suite of structural and modified proteins described above demonstrates a means
405 through which *P. antarctica*'s colonial morphotype could be constructed, and this dataset provides
406 rare molecular evidence for the proteome reconstruction needed to switch between single
407 organisms to a multicellular colony. The evolution of multicellularity in Eukaryotes is an area of
408 significant interest that has mostly focused on model organisms with colonial forms such as

409 Choanoflagellates and *Volvox* (Abedin and King, 2010). Genomic studies of the former identified
410 the presence of protein families involved in cell interactions within metazoans, including C-type
411 lectins, cadherins, and fibrinogen (King et al., 2003). In other lineages of microalgae that form
412 colonial structures, such as *Volvox carteri*, there is supporting evidence for glycoproteins cross-
413 linking within the extracellular matrix of colonies (Hallmann, 2003), as well as serving other
414 important functional roles in cell-cell attachment during colony formation (for example, colony
415 formation in the cyanobacteria *Microcystis aeruginosa*) and as an integral component of cell walls
416 (for example, the diatoms *Navicula pelliculosa* and *Craspedostauros australis*) (Chiovitti et al.,
417 2003; Kröger et al., 1994; Zilliges et al., 2008). In this study, environmental isolates of *P.*
418 *antarctica* displayed consistent trends in similar protein families (for example, lectins, fibrillins,
419 and glycoproteins), and they were produced at higher levels under elevated iron conditions when
420 strain 1871 was primarily in colonial form. Given *P. antarctica*'s environmental importance and
421 an ability to control the transition between flagellates and colony cell types through iron
422 availability, *P. antarctica* may serve as a useful model for studying multicellularity in nature and
423 in the context of environmental change.

424 In contrast to these putative colonial structural proteins, there were canonical cytoskeletal
425 proteins such as actin and tubulin observed in *P. antarctica* cultures grown under low iron
426 conditions (Supplementary Fig. 1). These proteins were likely associated with the flagella and the
427 haptonema, a shorter organelle containing nine microtubules that is characteristic of Haptophytes
428 (Zingone et al., 1999), found in the solitary *Phaeocystis* cell, and similar to other eukaryotic
429 flagellar systems such as *Chlamydomonas* (Watanabe et al., 2004). Additionally, a suite of proteins
430 with calcium-binding domains (EF-hand protein families) was identified in greater relative
431 abundance under low iron growth conditions in both strains (Fig. 5; Supplementary Fig. 1 and

432 Supplementary Data 1). In diatoms, calcium-signaling mechanisms have been directly linked with
433 how cells respond to bioavailable iron, as well as stress responses (Allen et al., 2008; Vardi, 2008).
434 Calcium (and magnesium) ions also play an integral role in the ability for extracellular mucus to
435 gel (van Boekel, 1992). The greater abundance of putative calcium-binding proteins under low
436 iron conditions suggests an important role for intracellular calcium, either in its involvement in
437 flagellate motility and/or having a role in inhibiting the cells' abilities to form colonies while under
438 iron limitation. This use of calcium signaling is notable given that calcium is a major constituent
439 of seawater (0.01 mol L^{-1}), implying a need for efflux and exclusion of calcium from the
440 cytoplasm.

441

442 **3.5 *Phaeocystis antarctica* strain-specific responses**

443 *Phaeocystis antarctica* is believed to have speciated from warm-water ancestors, and populations
444 within the Antarctic are mixed via the rapid Antarctic Circumpolar Current (ACC, 1-2 years)
445 circulation with the Ross Sea and Weddell Sea, which entrains strains nearly simultaneously
446 (Lange et al., 2002). However, given the original geographic location of the isolates, there may be
447 some differences regarding adaptation and ecological role between strains. In the Ross Sea, *P.*
448 *antarctica* dominates, and cells exhibit seasonal variability between flagellated states (early
449 Spring, late summer) and colonial stage (late Spring/early summer) (Smith et al., 2003). In
450 contrast, in the Western Antarctic Peninsula, near the Weddell Sea where strain 1871 was isolated
451 from (Palmer station), *P. antarctica* is outnumbered by diatoms and cryptomonads in terms of
452 algal biomass, and colonies are generally rare (Ducklow et al., 2007). While global proteomic and
453 transcriptomic analyses revealed differences among strains (Supplementary Data 1), both strains
454 had responses that overwhelmingly supported a concerted effort towards structural changes under

455 high iron versus low iron, consistent with the minor phylogenetic differences previously reported
456 for *P. antarctica* isolates due to rapid ACC circulation (Lange et al., 2002).

457

458 **3.6 Examination of a *Phaeocystis* bloom metaproteome from the Ross Sea**

459 The detailed laboratory studies above can be compared to a first metaproteomic analysis
460 of a Ross Sea *Phaeocystis antarctica* bloom to provide an examination of the *in situ* ecology and
461 biogeochemical and their underlying biochemical signatures. Due to the newness of
462 metaproteomic eukaryotic phytoplankton research, some methodological detail has been
463 incorporated into this section. For field analysis a net tow sample was collected north of Ross
464 Island (Fig. 8) on December 30th 2005, in which *Phaeocystis* colonies were visually dominant.
465 Temporal changes in the bloom composition have been described for this summer expedition and
466 an austral spring expedition later that year (NBP06-01 and NBP06-08, respectively), and a shift
467 was observed from a *P. antarctica* dominated ecosystem to a mixture of *P. antarctica* and diatoms
468 (Smith et al., 2013). Surface pigment distributions showed the sampling region to be within a
469 particularly intense bloom dominated by *Phaeocystis* as observed by abundant 19'-
470 hexanoyloxyfucoxanthin pigment (Fig. 8), reaching concentrations of 1096 ng L⁻¹ and total
471 chlorophyll *a* concentrations of 1860 ng L⁻¹ on the sampling day. CHEMTAX analysis of these
472 HPLC pigments found that *P. antarctica* populations accounted for approximately 88% of surface
473 water total chlorophyll at this time. Fucoxanthin pigment, characteristic of diatoms, was lower
474 here (136 ng L⁻¹) compared to samples from the western Ross Sea (Fig. 8), consistent with prior
475 Ross Sea observations. Repeated sampling near the sampling region (~77.5°S) two weeks after
476 taking the metaproteome sample found lower overall chlorophyll *a* levels (Smith et al., 2013),
477 consistent with bloom decay. Iron measured very near this location (76.82° S, 170.76° E also on

478 December 30, 2005), found a surface dissolved iron concentration of 170pM (6m depth) and an
479 acid-labile particulate iron concentration of 1590 pM (Sedwick et al., 2011), consistent with iron
480 depletion in seawater following drawdown of the accumulated winter iron supply and
481 incorporation of iron into biological particulate material (Noble et al., 2013; Sedwick et al., 2000).

482 The metaproteome analyses of the Ross Sea sample were conducted by bottom-up mass
483 spectrometry analysis of tryptic peptides using initially a 1-dimension and subsequently a deeper
484 2-dimension chromatographic methodology (1D and 2D hereon), followed by peptide-to-spectrum
485 matching of putative peptide masses and their fragment ions to predicted peptides from translated
486 DNA sequences. While this approach is common for model organisms and has been successfully
487 applied to primarily prokaryotic components of natural communities (Morris et al., 2010; Ram et
488 al., 2005; Sowell et al., 2008; Williams et al., 2012), there continue to be challenges in
489 metaproteomics analyses of diverse communities particularly when including an extensive
490 eukaryotic component such as is present in the Ross Sea phytoplankton bloom. VerBerkmoes et
491 al. (2005) demonstrated the feasibility of using mass spectrometry metaproteomic analysis for the
492 detection of eukaryotic proteins in a complex sample matrix. To address these issues, we utilized
493 three sequences databases for peptide-to-spectrum matching (see Methods and Supplementary
494 Information Table S2). Analysis of both unique (tryptic) peptides and identified proteins are
495 provided here, where unique peptides are particularly valuable in metaproteome interpretation as
496 a basal unit of protein diversity that can be definitively compared across the three sequence
497 databases (Saito et al., 2015).

498 The combined *P. antarctica* strain transcriptome database (Database #1) generated the
499 largest number of protein and unique peptide identifications 1545 and 3816 in 2D, (912 and 2103
500 in 1D), respectively (Table 2, Fig. 9a). This strong relative performance of the strain database was

501 surprising, and likely reflects the depth of the *P. antarctica* isolate transcriptomes and resultant
502 translation into greater metaproteomic depth. Approximately sixty percent of field identifications
503 mapped to strain 1374 (57%); a broad synthesis of all proteomes based on KOG annotations also
504 indicated that the metaproteomes appeared most similar to the Ross Sea strain 1374
505 (Supplementary Fig. 3). The Ross Sea metatranscriptome database (Database #2) resulted in 1475
506 proteins and 3210 unique peptides in 2D analyses (859 proteins and 1520 unique peptides in 1D)
507 distributed across a large number of taxa, with 324 of those proteins associated with *P. antarctica*.
508 The Antarctic bacterial metagenome database (Database #3) produced 102 proteins and 237 unique
509 peptides in 2D (98 proteins and 186 peptides in 1D) that mapped to bacteria likely associated with
510 the phytoplankton communities, given the use of a net that would not otherwise capture free-living
511 bacteria. The low number of bacterial protein and peptides identifications could reflect their small
512 abundance or limited metagenomic coverage. Due to the extensive diversity present, there was
513 overlap between the peptide identifications from each database for the 5885 total unique peptides
514 in 2D (3193 in 1D) : 1222 (in 2D; 544 in 1D) *P. antarctica* peptides were shared between the
515 *Phaeocystis* strain and Ross Sea metatranscriptome databases, 158 (in 2D; 69 in 1D) bacterial
516 peptides were in common between the Ross Sea metatranscriptome and the bacterial metagenomic
517 databases, followed by very small numbers shared between bacterial metagenome and the
518 *Phaeocystis* strains database searches (8 peptides in both 1D and 2D), and all three databases (7
519 and 4 peptides in 1D and 2D, respectively), likely due to a small fraction of tryptic peptides shared
520 between diverse organisms (Saito et al., 2015).

521 This multi-database approach and the relatively low overlap illustrates the necessity of
522 employing diverse sequence databases that target distinct components of the biological
523 community, as well as the value in coupling metatranscriptomic and metagenomic sequence

524 databases to metaproteomic functional analysis to capture the extent of natural diversity. This is
525 evident in the taxon group analysis, where the metatranscriptome has a large representation of
526 Dinophyta and diatoms and only a small contribution from Haptophyta that include *Phaeocystis*,
527 likely due to the large genome sizes and transcription rates, particularly of dinoflagellates, and
528 perhaps due to interferences of *Phaeocystis* RNA extraction due to the copious mucilage present
529 (Fig. 9b). In contrast the metaproteome derived from the metatranscriptome database is dominated
530 by Haptophyta and Dinophyta, with minor contributions from other groups (Fig. 9d), reflecting
531 the dominant organismal composition seen in the pigment analyses (Fig. 8). Due to a coarse net
532 mesh size much larger than a typical bacterial cell, the bacterial community captured by these
533 metatranscriptome and metaproteome analyses most likely reflects the microbiome associated with
534 larger phytoplankton and protists, particularly within the abundant *P. antarctica* colonies.
535 Database #2 and #3 result in 211 and 102 bacterial protein identifications (in 2D; 148 and 100 in
536 1D), respectively, including representatives from *Oceanospirillaceae*, *Rhodobacteraceae*,
537 *Cryomorphaceae*, *Flavobacteria*, and *Gamma proteobacteria* (Fig. 9c and d). The lower number
538 of bacterial identifications could be due to low bacterial biomass in the net tow sample relative to
539 phytoplankton biomass and/or limited metagenomics coverage.

540 Together this Ross Sea bloom metaproteome-metatranscriptome analysis provides a
541 window into the complex interactions of this community with its chemical environment.
542 *Phaeocystis antarctica* proteins were abundant in the sample with over 450 (in 2D; 300 in 1D)
543 proteins identified, yet interestingly, we identified proteins associated with both high and low iron
544 treatments, including those corresponding to flagellate and colonial life stages identified in the
545 culture experiments (Fig. 10 and Supplementary Fig. 1). This presence of both life cycle stages of
546 *Phaeocystis* could be interpreted as evidence of an actively growing bloom, with growing

547 flagellate cells coalescing to form new colonies, as well as a standing stock of colonial cells. As
548 mentioned earlier, division and growth of *P. antarctica* colonies is believed to require transitioning
549 back through the flagellate life cycle stage, hence a mixed population of flagellate and colonial
550 stages would be expected of a growing population, consistent with our laboratory observations
551 (Fig. 3c).

552 The presence of well-known iron-sparing proteins such as plastocyanin (Fig. 10) was
553 consistent with the depleted dissolved iron concentration (170 pM) in nearby surface waters that
554 are closest to the 120 pM Fe' of the low iron treatments (Peers and Price, 2006; Sedwick et al.,
555 2011), as well as incubation experiments on the same expedition initiated three days prior that
556 demonstrated iron limitation of *P. antarctica* (and iron-B₁₂ colimitation of diatom) populations
557 (Bertrand et al., 2007). Notably, the actual Fe' of the Ross Sea was likely considerably lower than
558 this due to the presence of strong organic iron complexes (Boye et al., 2001). Strzepek et al. found
559 evidence for growth of *P. antarctica* and some polar diatoms on strong organic iron complexes at
560 somewhat reduced growth rates in their culture experiments, implying a high-affinity iron
561 acquisition system such as a ferric reductase, although the molecular components of such a system
562 have yet to be identified in *P. antarctica* (Strzepek et al., 2011). As described above, it is likely
563 that both flagellate and colonial cell types have a need to manifest iron stress responses (e.g.
564 distinct ISIP proteins found in the flagellate and colonial dominated cultures, Figs. 5 and 6), and
565 that those distinct responses may be based on the extensive physical differences between life cycle
566 phenotypes. The low contribution of chain-forming diatoms to this metaproteome sample was
567 consistent with the higher sensitivity of some Ross Sea diatom strains to iron stress such as
568 *Chaetoceros* (Fig. 3d) and the low iron availability. Careful examination of targeted mass
569 spectrometry results (precursor and fragment ion analysis) for select iron proteins identified in

570 culture studies showed consistently high quality chromatograms within the field sample,
571 demonstrating a capability to measure these potential peptide biomarkers within complex
572 environmental samples in future field studies characterizing bloom and biogeochemical dynamics
573 (Fig. 11 and Supplementary Figs. 4-10).

574 The metaproteome analyses also captured relevant functional elements of the bacterial
575 microbiome associated with the eukaryotic community, based on the bacterial proteins identified
576 in both the bacterial databases and the Ross Sea metatranscriptome (Fig. 9c and 9d). For example,
577 the SAR92 clade of proteorhodopsin-containing heterotrophic bacteria was present (Stingl et al.,
578 2007), and expressed both the iron storage protein bacterioferritin and TonB receptors, the latter
579 of which are involved in siderophore and B₁₂ transport. In addition, the Fur iron regulon, iron-
580 requiring ribonucleotide reductase, as well as the vitamin related CobN cobalamin biosynthesis
581 protein, B₁₂-requiring methyl-malonyl CoA, and thiamine ABC transporter were observed from
582 several heterotrophic bacteria species including *Oceanospirillaceae*, *Rhodobacteraceae*, and
583 *Cryomorphaceae* (Supplementary Data 2) (Bertrand et al., 2015; Murray and Grzymalski, 2007).
584 These results imply that heterotrophic bacteria known to be associated with the *Phaeocystis*
585 colonies, such as SAR92 and *Oceanospirillaceae*, were also likely responding to micronutrients
586 by concentrating and storing iron, and through biosynthesis of B₁₂. In doing so this bacterial
587 microbiome could have been harboring an “internal” source of the micronutrients, fostering a
588 mutualism with *Phaeocystis* colonies in exchange for a carbon source and consistent with the high
589 particulate iron measured during this station (Sedwick et al., 2011). Together this could create a
590 competitive advantage for *P. antarctica* relative to the iron and B₁₂-stressed diatoms for early
591 season bloom formation, as previously hypothesized and observed in the Ross Sea in enrichment
592 studies (Bertrand et al., 2007). Although diatoms were less prominent in the dataset, several diatom

593 proteins identified were indicative of the potential for iron stress (e.g., plastocyanin and ISIP3;
594 Supplementary Data 2); however, the diatom CBA1 cobalamin acquisition protein was not
595 identified in the metatranscriptome, and hence would not be detected in the metaproteome using
596 the current methods, but could be targeted in future studies from this dataset.

597

598 **4. Conclusions**

599 *Phaeocystis antarctica* is a major contributor to Southern Ocean primary productivity, yet
600 arguably is one of the least well understood of key marine phytoplankton species. The multiple
601 life cycle stages of *P. antarctica* add to its ecological and biochemical complexity. Here we have
602 undertaken a detailed combined physiological and proteomic analysis enabled by transcriptomic
603 sequencing under varying conditions of iron nutrition, and compared these to an initial study of
604 the metaproteome of a Ross Sea *Phaeocystis* bloom. These results demonstrate that *P. antarctica*
605 has evolved to utilize elaborate capabilities to confront the widespread iron scarcity that occurs in
606 the Ross Sea and Southern Ocean, including iron metalloenzyme sparing systems and the
607 deployment of transport and other systems that appear to be unique to the flagellate and colonial
608 morphotypes. To our surprise, increasing iron abundance triggered colony formation in one strain
609 in this study, and visual and proteomic evidence implied the second strain was also attempting to
610 do so. Prior studies have invoked light irradiance and mixed layer depth as key factors in colony
611 production and the concurrent Ross Sea *P. antarctica* bloom initiation (Arrigo et al., 1999), and
612 hence there may be other factors that could have this effect as well. These results also provide
613 preliminary insight into the cellular restructuring processes that occurs upon cellular
614 metamorphosis between life cycle stages in *P. antarctica*, as well as identifying numerous dynamic
615 proteins of unknown function for future study. Finally, this study demonstrates the potential for

616 the application of coupled transcriptomic and proteomic biomarker methodologies in studying the
617 ecology of microbial interactions (including iron and B₁₂) and their influence on biogeochemistry
618 in complex polar ecosystems such as the Ross Sea. The improved molecular and biochemical
619 understanding of *P. antarctica* and its response to iron provided here are valuable in the design of
620 future experiments and targeted metaproteomic assays to examine natural populations and to
621 improve understanding of environmental factors that influence the annual bloom formation of an
622 important coastal ecosystem of the Southern Ocean.

623

624

625 **Acknowledgements**

626 Support for this study was provided by an Investigator grant to M. Saito from the Gordon and
627 Betty Moore Foundation (GBMF3782), and National Science Foundation grants NSF-PLR
628 0732665, OCE-1435056, OCE-1220484, the WHOI Coastal Ocean Institute, and a CINAR
629 Postdoctoral Scholar Fellowship provided to S. Bender through the Woods Hole Oceanographic
630 Institution. Support was provided to A. Allen through NSF awards ANT-0732822, ANT-1043671,
631 OCE-1136477, and Gordon and Betty Moore Foundation grant GBMF3828. Additional support
632 was provided to GRD through NSF award, OPP-0338097. We are indebted to Roberta Marinelli
633 for her leadership and vision. We would also like to thank Emily Lorch for her assistance with
634 culturing, Julie Rose for generously sharing a net tow field sample, and Andreas Krupke for
635 manuscript feedback.

636

637 **Author Contributions**

638 S.J.B. contributed to data analysis and writing; D.M.M. conducted the laboratory experiments and
639 (meta)proteome extractions; M.R.M. conducted the mass spectrometry sample preparation and
640 processing; H.Z. conducted RNA extractions; J.P.M. and J.B. contributed to transcriptome
641 sequence analyses; G.R.D. contributed to field measurements and manuscript edits; A.E.A.
642 contributed to the experimental design, data analysis, and writing; M.A.S. contributed to
643 experimental design, data analysis, and writing.

644 **Financial Conflicts:** The authors have no financial conflicts involving the research presented in
645 this manuscript.

646

647 **Table 1.** Comparison of the total number of proteins and spectra measured in the proteome for
648 each strain/treatment along with the number of differentially expressed transcripts between select
649 conditions for *P. antarctica* strain 1871 and strain 1374. Proteins were identified using a 1% FDR
650 (false discovery rate) threshold, a peptide threshold of 95%, and a minimum of 2 unique peptides
651 per protein. The total number of peptide-to-spectrum matches (PSMs) is given for the total of each
652 strain in parentheses. A threshold of 3 spectral counts in at least one of the treatments was selected
653 for inclusion in the comparative analysis.

654

Strain	Treatment (Fe' pM)	Proteins Identified (PSMs)
1871	2	204
	41	214
	120	234
	740	226
	1200	251
	3900	258
	Total	536 (28887)
1374	2	581
	41	613
	120	600
	740	654
	1200	623
	3900	527
	Total	1085 (72087)

655 **Table 2.** Comparison of the total number of proteins, peptides, and spectra measured in the
 656 Ross Sea metaproteome net tow sample using three databases for peptide-to-spectrum
 657 matching (see Table S2). Results from 2-dimension and 1-dimension (1D in parentheses)
 658 analyses are shown.

Peptide-to-spectrum - matching database	Total proteins	Total Unique Peptides	Total spectra matched	Decoy FDR ⁺ Percent (peptide level)
1) <i>Phaeocystis</i> strains transcriptomes*	1545 (912)	3816 (2103)	14088 (8226)	0.6 (0.17)
2) Ross Sea metatranscriptome**	1474 (859)	3210 (1520)	10154 (4725)	0.1 (0.7)
3) Antarctic bacterial metagenomes***	102 (92)	237 (186)	530 (440)	3.6 (2.3)

659

660 ⁺FDR refers to false discovery rate of a reversed peptide database

661

662 * Metaproteome annotated using the laboratory-generated transcriptomes for strain 1871
 663 and strain 1374 (database #1).

664

665 ** Metaproteome annotated using the metatranscriptome generated from sample split of
 666 original Ross Sea sample (database #2).

667

668 *** Bacterial metaproteome annotated using bacterial metagenomes from Delmont et al.,
 2014 (database #3).

669

670

667 **Figure Legends**

668 **Figure 1.** Micrographs of (a) a single *Phaeocystis* in cell culture, and (b) *Phaeocystis* colonies in
669 a Ross Sea bloom.

670

671 **Figure 2.** Experimental workflow used in this study. Culture and field samples (top),
672 transcriptome analyses (2nd row), sequence database construction for proteomics (3rd row), and
673 proteomic and metaproteomic analyses (bottom row).

674

675 **Figure 3.** The effect of iron concentration on colony formation and cell physiology in two strains
676 of *P. antarctica* – 1871 and 1374. Growth rates collected from acclimated culture stocks prior to
677 the start of the experiments (*a*, strain 1871; *b*, strain 1374), calculated using relative fluorescence
678 units from three transfers of acclimated cultures (error bars indicate SD, n=3). Accompanying
679 gray bars represent growth rates calculated based on cell counts made during the course of the
680 proteome-harvest experiments (n=1). (*c*) The number of *P. antarctica* 1871 free-living cells
681 (gray bars) compared to cells associated with colonies (black bars) showed a shift to a majority
682 of colonial cells when $Fe' \geq 740$ pM. (*d*) Growth rate of Ross Sea diatom isolate *Chaetoceros* sp.
683 strain RS-19 in the same media compositions (n=1), demonstrated a higher sensitivity to iron
684 scarcity and a lack of iron contamination in the media. Cell size for strain 1871 (*e*; black circles)
685 and strain 1374 (*f*; white circles); error bars represent SD of n=20 cell measurements per
686 treatment.

687

688 **Figure 4.** Principle Component Analysis (PCA) of the measured proteomes for each iron
689 condition for strain 1871 and strain 1374 and corresponding line graphs highlighting the proteins

690 driving the PCA separation (PCA analyses: ≥ 0.9 or ≤ -0.9). (*a* and *d*) Iron treatments (pM Fe³⁺)
691 are highlighted by color (2, black; 41, red; 120, orange; 740, green; 1200, purple; 3900, blue) and
692 large ellipses indicate confidence ellipses calculated using the R package, FactorMineR. Each
693 small, solid circle represents a technical replicate per iron treatment (n=3); colored, open squares
694 represent the mean of the iron treatment (empirical variance divided by the number of
695 observations). Proteins with Eigen values ≥ 0.9 or ≤ -0.9 are plotted in graphs b and c for strain
696 1871 and *e* and *f* for strain 1374 to highlight the subset of proteins driving the variance in
697 Dimension 1. Individual protein spectral counts normalized to total spectral counts for all
698 treatments for a given protein, written as “normalized relative protein abundance” are plotted on
699 the y-axis. The six iron treatments (pM Fe³⁺) are plotted from low to high (left to right) on the x-
700 axis.

701

702 **Figure 5.** Heatmaps highlighting the relative protein abundance for the six treatments for *P.*
703 *antarctica* strain 1871 (*a*) and strain 1374 (*b*). The darker green color indicates a greater relative
704 abundance compared to the purple treatments. The “shared abundance patterns” column features
705 a check-mark when a shared response to changes in iron availability between the relative protein
706 abundance and the transcript abundance was observed (for example, both transcripts and proteins
707 have a higher abundance under high iron compared to low iron growth [or] both transcripts and
708 proteins have a higher abundance under low iron compared to high iron growth). The “field
709 presence” column indicates whether or not that protein was detected in the field metaproteome
710 (annotated using Database #1). Protein annotations are based on KEGG, KOG, and PFam
711 descriptions. Annotations in red are associated with iron metabolism and those in blue, cell
712 adhesion/structure.

713

714 **Figure 6.** Examination of iron stress response proteins in *P. antarctica* strain 1871 (top) and
715 1374 (bottom). Relative protein abundance is shown as normalized spectral counts, where
716 spectral counts have been normalized across experiment treatments for each strain, but not to the
717 maximum of each protein as used in prior figures to allow comparison of abundance for similar
718 isoforms. Error bars indicate the standard deviation of technical triplicate analyses.

719

720 **Figure 7.** Scatterplots of relative transcript abundance (y-axis) and relative protein abundance
721 (x-axis) for *P. antarctica* strain 1871 (a) and strain 1374 (b) for a high iron treatment (3900 pM
722 Fe³⁺) relative to a low iron treatment (41 pM Fe³⁺). Gray circles represent instances where
723 transcript abundance was not significantly different between conditions ($P \geq 0.99$). Quadrants
724 where relative protein and transcript abundances agree (upper right, lower left) and disagree
725 (upper left, lower right) are noted, as are select genes exhibiting the greatest relative protein
726 abundance and/or transcript abundance under a given treatment.

727

728 **Figure 8.** Location of the metaproteome sample and pigment data from a Ross Sea *Phaeocystis*
729 bloom net tow sample. (a) Station map of NBP06-01 (December 27, 2005 to January 23, 2006)
730 and the metaproteome sample was taken on December 30th by net tow location (red circle). (b)
731 19'-hexanoyloxyfucoxanthin ("19'-Hex") pigment is associated with *Phaeocystis*, while (c)
732 peridinin and (d) fucoxanthin pigments are typically associated with dinoflagellates and diatoms,
733 respectively (although dinoflagellates living heterotrophically can be lacking in pigment).
734 Comparisons of the spring and summer expeditions (NBP06-08 and NBP06-01, respectively),

735 observed a shift from being dominated by *P. antarctica* to being a mixture of *P. antarctica* and
736 diatoms. See Smith et al., 2013 for further details (Smith et al., 2013).

737

738 **Figure 9.** (a) Venn diagram of the attribution of the 5885 total unique peptides identified in the
739 metaproteome sample to three DNA/RNA sequence databases (Supplementary Table 2). (b)
740 Taxon group composition of genes identified by metatranscriptome analyses (combining Total
741 RNA and PolyA RNA fractions). (c) Taxon group composition of proteins identified by the
742 bacterial metagenomic database (Database #3). (d) Taxon group composition of proteins
743 identified by metatranscriptome database (Database #2).

744

745 **Figure 10.** Putative biomarkers identified in the *Phaeocystis* metaproteome annotated using the
746 field metatranscriptome (error bars represent SD of replicate samples; n=2; 1D dataset used).
747 Green bars indicate putative “low iron” biomarkers; red bars indicate putative “high iron”
748 biomarkers, and correspond to the life cycle stages observed (Fig. 3).

749

750 **Fig. 11.** Example spectra and chromatograms of fragment ions for two peptides corresponding to
751 a *P. antarctica* flavodoxin identified from the Ross Sea metaproteome sample (peptide sequences
752 found within Database #1, 1871, contig_31444_1_606_+, 1374 contig_202625_47_661_+; and,
753 Database #2 contig_175060_39_653_+). Peptide fragmentation spectra are shown in (a) and (c)
754 and example chromatograms of MS1 intensities as well as with +1 and +2 mass addition for
755 isotopic distributions is shown (b) and (d), demonstrating the utility of these iron stress biomarkers
756 in field samples.

757

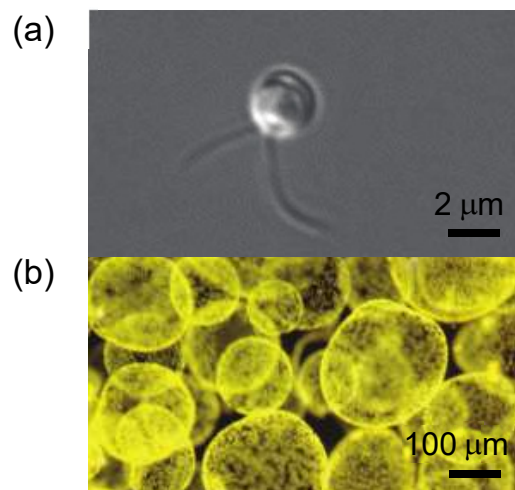
758

759 **Figure 1.**

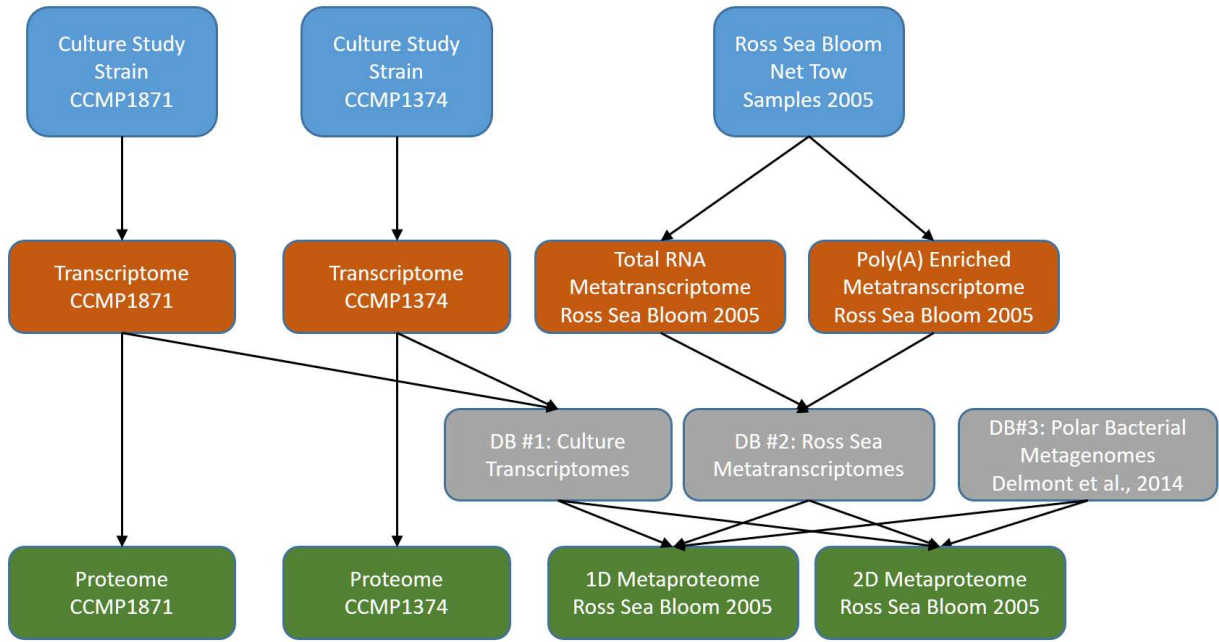
760

761

762

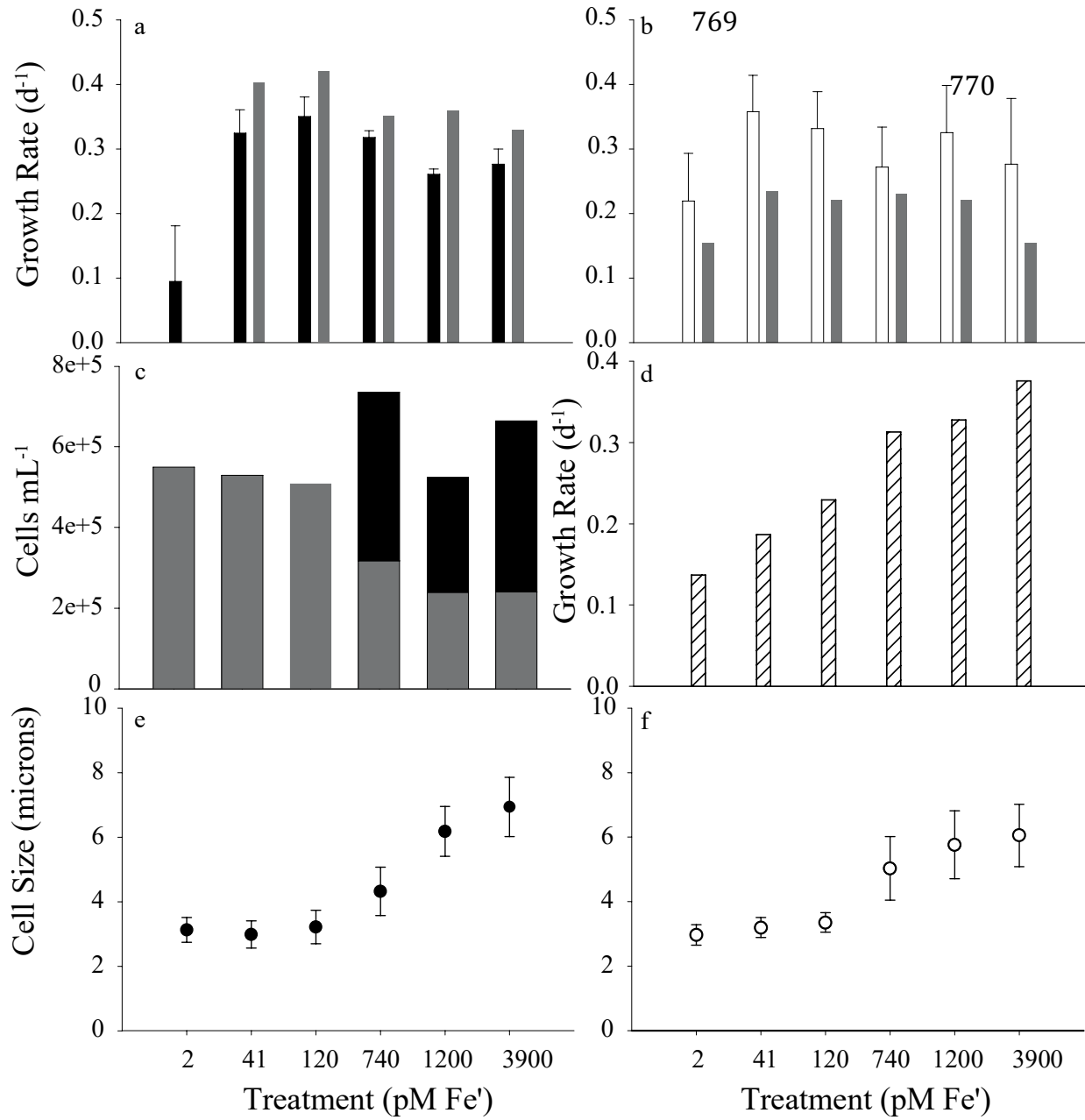


763 **Figure 2.**
764

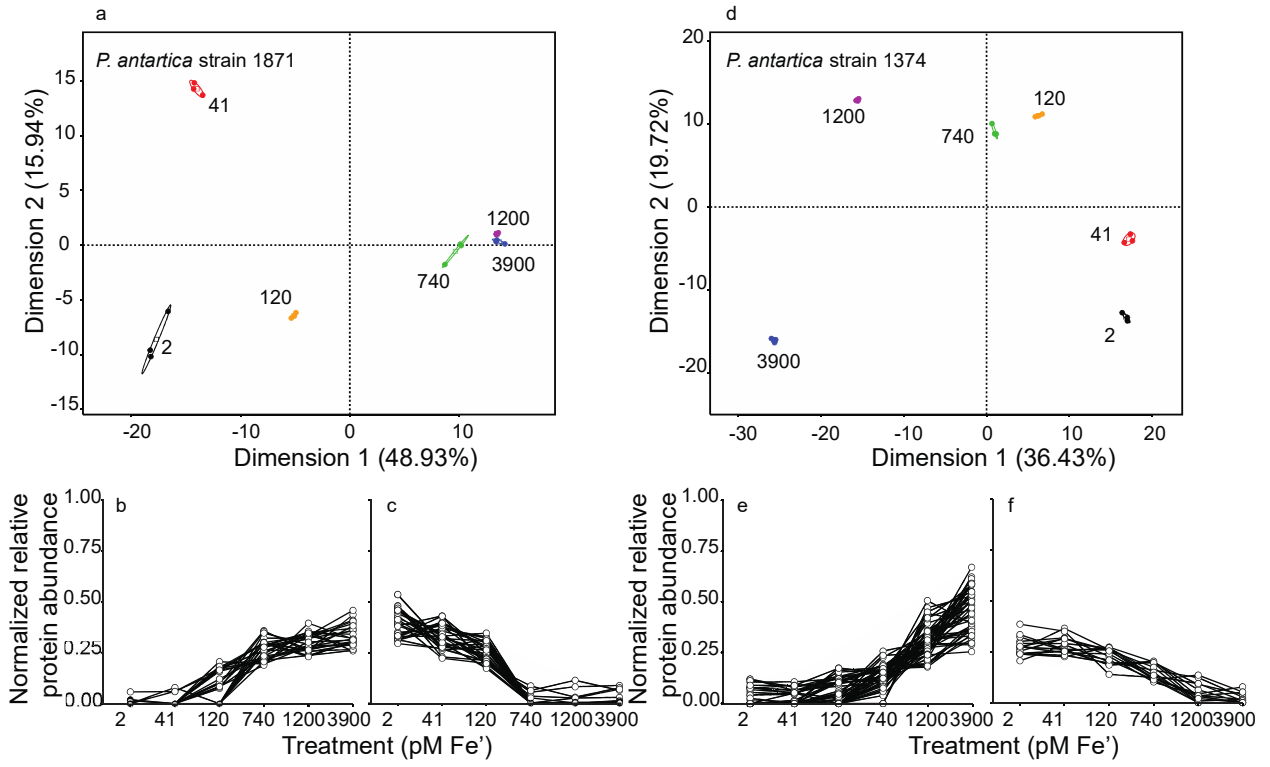


765

766 **Figure 3.**
 767
 768

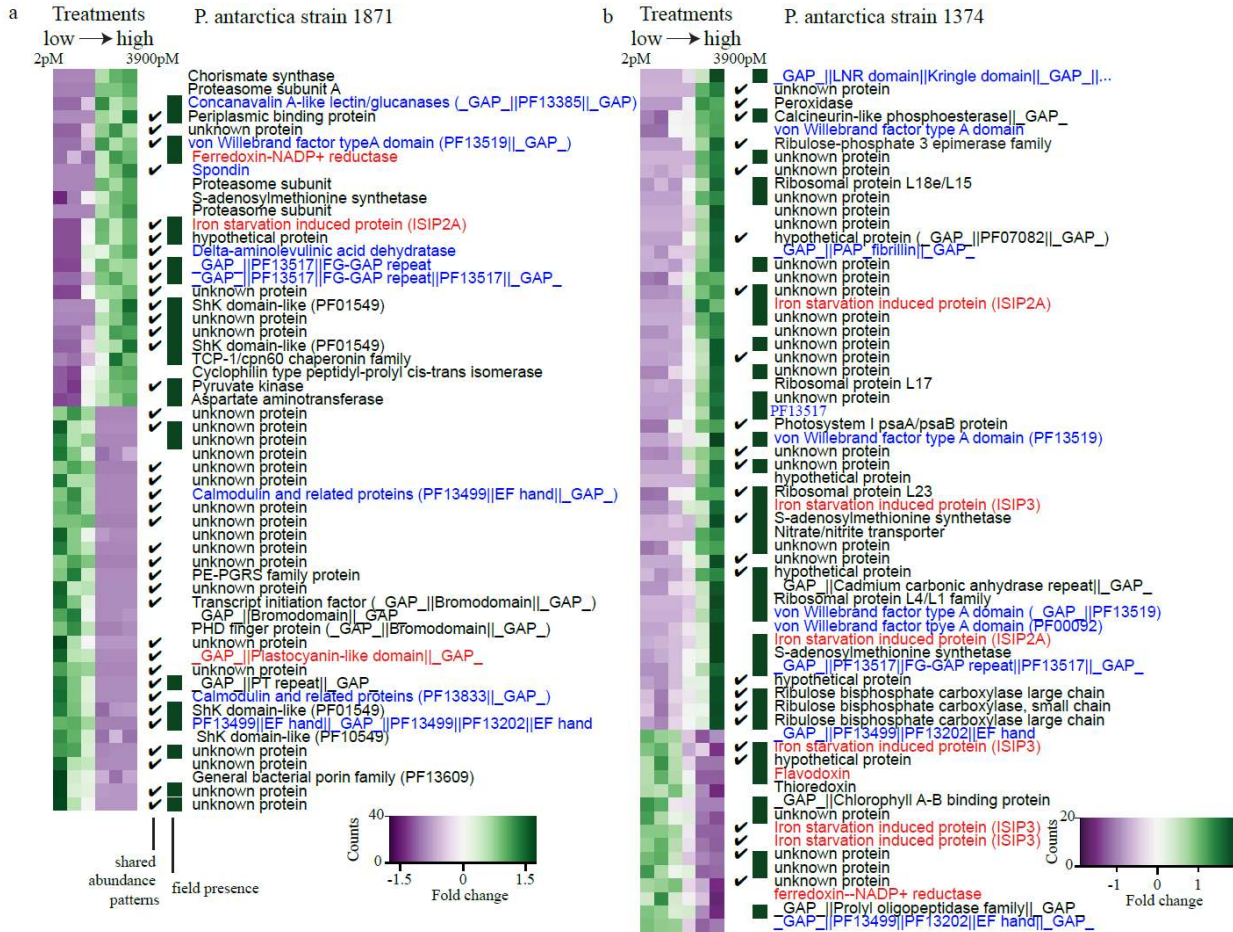


771 **Figure 4.**



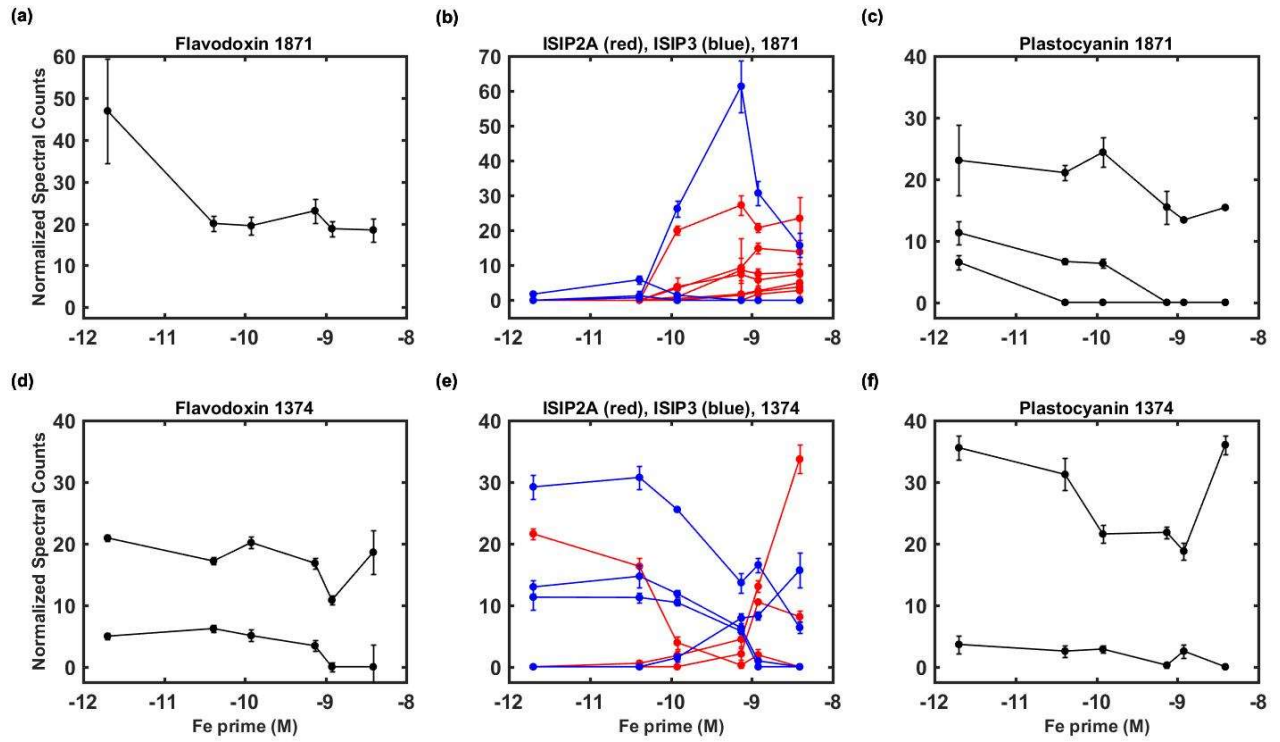
772
773
774

Figure 5.



775

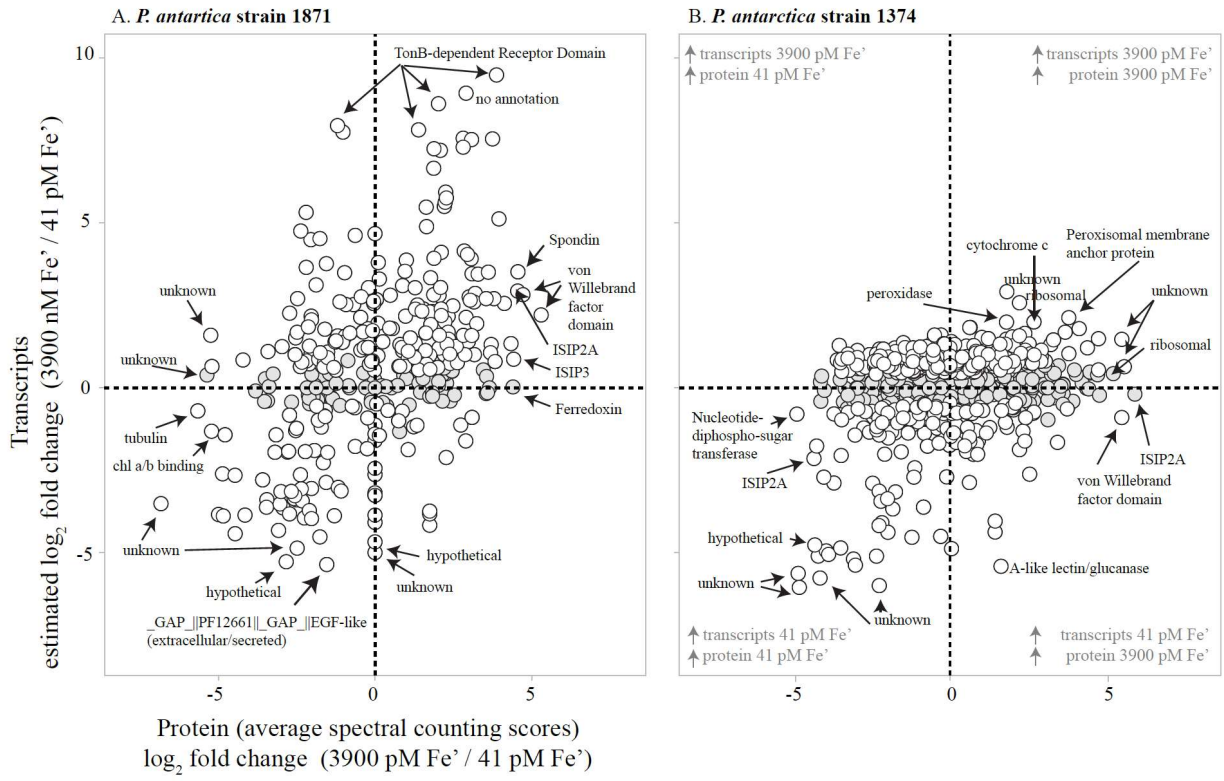
776 **Figure 6.**
777



778

779
780
781
782

Figure 7.



783

784

Figure 8.

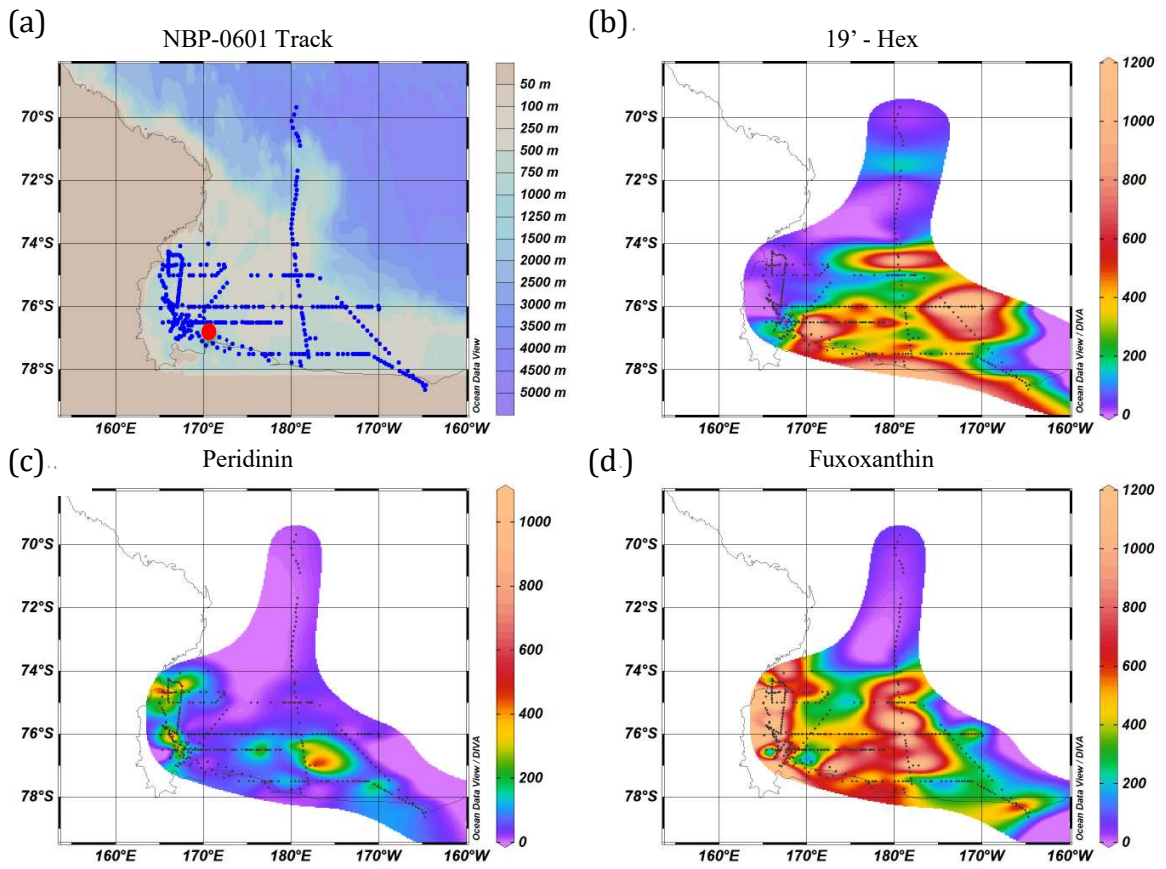
785

786

787

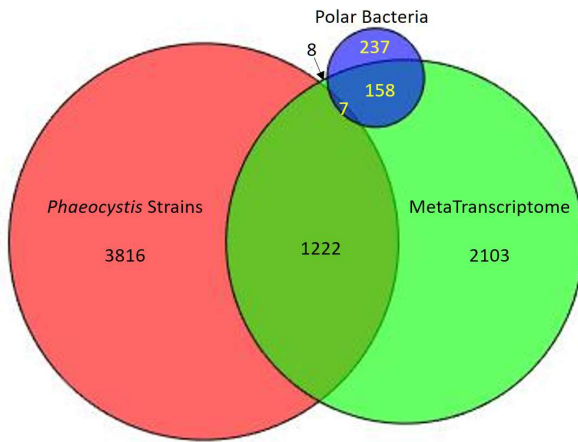
788

789

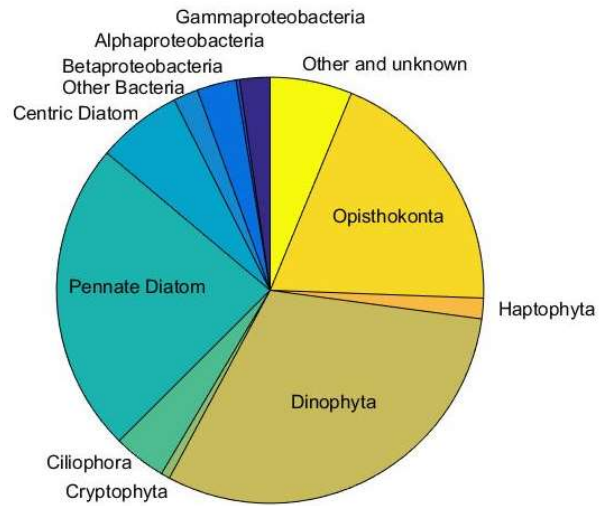


790 **Figure 9.**
 791

(a) Unique Peptides by Database

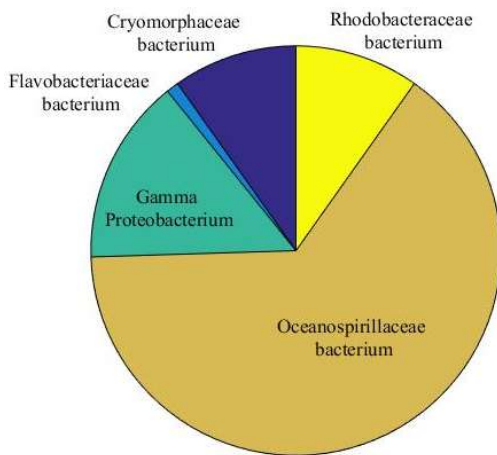


(b) Genes Identified by Metatranscriptome

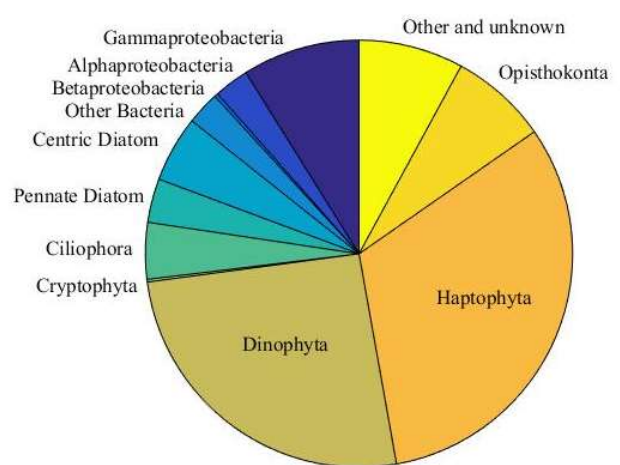


792

(c) Proteins by Bacterial Metagenome



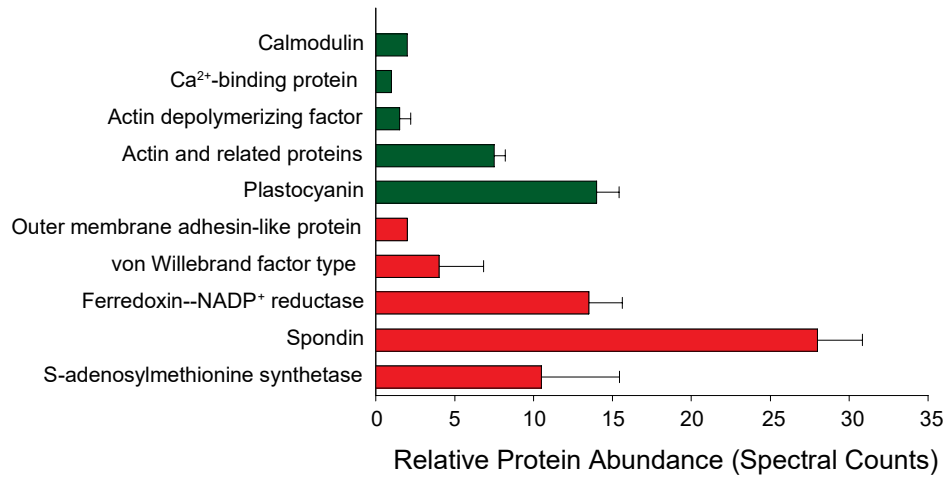
(d) Proteins Identified by Metatranscriptome



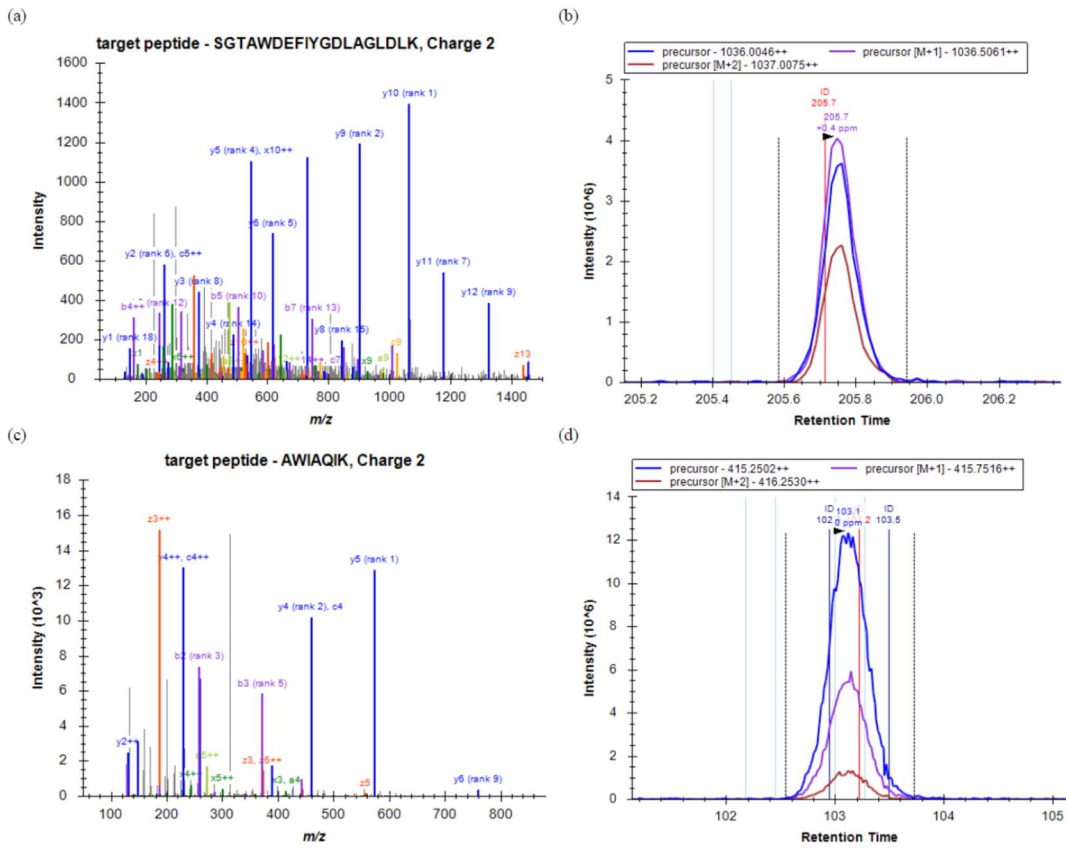
793

Figure 10.

794



795 **Figure 11.**
 796
 797



798

799 **References**

- 800 Abedin, M. and King, N.: Diverse and evolutionary paths to cell adhesion, *Trends in Cell*
801 *Biology*, 20(12), 734–742, 2010.
- 802 Alderkamp, A. C., Buma, A. G. J. and Van Rijssel, M.: The carbohydrates of *Phaeocystis* and
803 their degradation in the microbial food web, *Biogeochemistry*, 83, 99–118, 2007.
- 804 Allen, A. E., LaRoche, J., Maheswari, U., Lommer, M., Schauer, N., Lopez, P. J., Finazzi, G.,
805 Fernie, A. R. and Bowler, C.: Whole-cell response of the pennate diatom *Phaeodactylum*
806 *tricornutum* to iron starvation, vol. 105, pp. 10438–10443. 2008.
- 807 Arrigo, K. R., R, D. G., Dunbar, R. B., Robinson, D. H., vanWoert, M. L., Worthen, D. L. and
808 Lizotte, M. P.: Phytoplankton taxonomic variability in nutrient utilization and primary
809 production in the Ross Sea, *Journal of Geophysical Research*, 105(C4), 8827–8846,
810 doi:10.1029/1998JC000289, 2000.
- 811 Arrigo, K. R., Robinson, D. H., Worthen, D. L., Dunbar, R. B., R, D. G., vanWoert, M. L. and
812 Lizotte, M. P.: Phytoplankton community structure and the drawdown of nutrients and CO₂ in
813 the Southern Ocean, *Science*, 283, 365–367, doi:10.1126/science.283.5400.365, 1999.
- 814 Arrigo, K. R., Worthen, D., Schnell, A. and Lizotte, M. P.: Primary production in Southern
815 Ocean waters, *Journal of Geophysical Research*, 103(C8), 15587–15600, 1998.
- 816 Bertrand, E. M., McCrow, J. P., Moustafa, A., Zheng, H., McQuaid, J. B., Delmont, T. O., Post,
817 A. F., Sipler, R. E., Spackeen, J. L., Xu, K., Bronk, D. A., Hutchins, D. A. and Allen, A. E.:
818 Phytoplankton–bacterial interactions mediate micronutrient colimitation at the coastal Antarctic
819 sea ice edge, *Proceedings of the National Academy of Sciences*, 112(32), 9938–9943,
820 doi:10.1073/pnas.1501615112, 2015.
- 821 Bertrand, E. M., Moran, D. M., McIlvin, M. R., Hoffman, J. M., Allen, A. E. and Saito, M. A.:
822 Methionine synthase interreplacement in diatom cultures and communities: Implications for the
823 persistence of B₁₂ use by eukaryotic phytoplankton, *Limnology and Oceanography*, 58(4), 1431–
824 1450, doi:10.4319/lo.2013.58.4.1431, 2013.
- 825 Bertrand, E. M., Saito, M. A., Lee, P. A., Dunbar, R. B., Sedwick, P. N. and R, D. G.: Iron
826 limitation of a springtime bacterial and phytoplankton community in the Ross Sea: Implications
827 for Vitamin B₁₂ nutrition, *Frontiers in Microbiology*, 2, 1–12, doi:10.3389/fmicb.2011.00160,
828 2011.
- 829 Bertrand, E. M., Saito, M. A., Rose, J. M., Riesselman, C. R., Lohan, M. C., Noble, A. E., Lee,
830 P. A. and R, D. G.: Vitamin B₁₂ and iron colimitation of phytoplankton growth in the Ross Sea,
831 *Limnology and Oceanography*, 52(3), 1079–1093, 2007.
- 832 Boye, M., van den Berg, C., de Jong, J., Leach, H., Croot, P. and de Baar, H. J. W.: Organic
833 complexation of iron in the Southern Ocean, *Deep-Sea Research Part I*, 48(6), 1477–1497, 2001.
- 834 Chiovitti, A., Bacic, A., Burke, J. and Wetherbee, R.: Heterogeneous xylose-rich glycans are

- 835 associated with extracellular glycoproteins from the biofouling diatom *Craspedostauros*
836 *australis* (Bacillariophyceae), European Journal of Phycology, 38(4), 351–360,
837 doi:10.1080/09670260310001612637, 2003.
- 838 Coale, K. H., Wang, X., Tanner, S. J. and Johnson, K. S.: Phytoplankton growth and biological
839 response to iron and zinc addition in the Ross Sea and Antarctic Circumpolar Current along
840 170°W, Deep-Sea Research Part II, 50, 635–653, 2003.
- 841 Delmont, T. O., Hammar, K. M., Ducklow, H. W., Yager, P. L. and Post, A. F.: *Phaeocystis*
842 *antarctica* blooms strongly influence bacterial community structures in the Amundsen Sea
843 polynya, Frontiers in Microbiology, 5, 646, 2014.
- 844 DiTullio, G. R., Grebmeier, J. M., Arrigo, K. R., Lizotte, M. P., Robinson, D. H., Leventer, A.,
845 Barry, J. P., vanWoert, M. L. and Dunbar, R. B.: Rapid and early export of *Phaeocystis*
846 *antarctica* blooms in the Ross Sea, Antarctica, Nature, 404, 595–598, doi:10.1038/35007061,
847 2000.
- 848 Drake, J. L., Mass, T., Haramaty, L., Zelzion, E., Bhattacharya, D. and Falkowski, P. G.:
849 Proteomic analysis of skeletal organic matrix from the stony coral *Stylophora pistillata*,
850 Proceedings of the National Academy of Sciences, 110(10), 3788–3793, 2013.
- 851 Ducklow, H. W., Baker, K., Martinson, D. G., Quetin, L. B., Ross, R. M., Smith, R. C.,
852 Stammerjohn, S. E., Vernet, M. and Fraser, W.: Marine pelagic ecosystems: the West Antarctic
853 Peninsula, Philosophical Transactions of the Royal Society B, 362, 67–94,
854 doi:10.1098/rstb.2006.1955, 2007.
- 855 Dunbar, R. B., Leventer, A. R. and Mucciarone, D. A.: Water column sediment fluxes in the
856 Ross Sea, Antarctica: Atmospheric and sea ice forcing, Journal of Geophysical Research,
857 103(C13), 30741–30759, doi:10.1029/1998JC900001, 1998.
- 858 Dyhrman, S. T.: Identifying reference genes with stable expression from high throughput
859 sequence data,, 1–10, doi:10.3389/fmicb.2012.00385/abstract, 2012.
- 860 Eng, J. K., McCormack, A. L. and Yates, J. R.: An approach to correlate tandem mass spectral
861 data of peptides with amino acid sequences in a protein database, J Am Soc Mass Spectrom,
862 5(11), 976–989, doi:10.1016/1044-0305(94)80016-2, 1994.
- 863 Ewenstein, B. M.: Von Willebrand's disease, Annu. Rev. Med., 48(1), 525–542,
864 doi:10.1146/annurev.med.48.1.525, 1997.
- 865 Feng, Y., Hare, C. E., Rose, J. M., Handy, S. M., DiTullio, G. R., Lee, P. A., Smith, W. O., Jr,
866 Peloquin, J., Tozzi, S., Sun, J., Zhang, Y., Dunbar, R. B., Long, M. C., Sohst, B., Lohan, M. and
867 Hutchins, D. A.: Interactive effects of iron, irradiance and CO₂ on Ross Sea phytoplankton,
868 Deep-Sea Research Part I, 57, 368–383, doi:10.1016/j.dsr.2009.10.013, 2010.
- 869 Garcia, N. S., Sedwick, P. N. and DiTullio, G. R.: Influence of irradiance and iron on the growth
870 of colonial *Phaeocystis antarctica*: implications for seasonal bloom dynamics in the Ross Sea,
871 Antarctica, Aquatic Microbial Ecology, 57, 203–220, 2009.

- 872 Hallmann, A.: Extracellular matrix and sex-inducing pheromone in *Volvox*, in International
873 Review of Cytology, vol. 227, pp. 131–182, International Review of Cytology. 2003.
- 874 Hamm, C. E.: Architecture, ecology and biogeochemistry of *Phaeocystis* colonies, Journal of Sea
875 Research, 43, 307–315, 2000.
- 876 Hamm, C. E., Simson, D. A., Merkel, R. and Smetacek, V.: Colonies of *Phaeocystis globosa* are
877 protected by a thin but tough skin, Marine Ecology Progress Series, 187, 101–111, 1999.
- 878 Hayward, D. C., Hetherington, S., Behm, C. A., Grasso, L. C., Forêt, S., Miller, D. J. and Ball, E.
879 E.: Differential gene expression at coral settlement and metamorphosis - A subtractive
880 hybridization study, PLoS ONE, 6(10), e26411, doi:10.1371/journal.pone.0026411, 2011.
- 881 Jacobsen, A., Larsen, A., Martínez-Martínez, J., Verity, P. G. and Frischer, M. E.: Susceptibility
882 of colonies and colonial cells of *Phaeocystis pouchetii* (Haptophyta) to viral infection, Aquatic
883 Microbial Ecology, 48, 105–112, 2007.
- 884 King, N., Hittinger, C. T. and Carroll, S. B.: Evolution of key cell signaling and adhesion protein
885 families predates animal origins, Science, 301(5631), 361–363, doi:10.1126/science.1083853,
886 2003.
- 887 Kröger, N., Bergsdorf, C. and Sumper, M.: A new calcium binding glycoprotein family
888 constitutes a major diatom cell wall component, The EMBO Journal, 13(19), 4676–4683, 1994.
- 889 Lagerheim, G.: Ueber *Phaeocystis poucheti* (Har.) Lagerh., eine Plankton-Flagellate, Oeivers af
890 Vet Akad Foerhandl, 4, 277–288, 1896.
- 891 Lange, M., Chen, Y.-Q. and Medlin, L. K.: Molecular genetic delineation of *Phaeocystis* species
892 (Prymnesiophyceae) using coding and non-coding regions of nuclear and plastid genomes,
893 European Journal of Phycology, 37(1), 77–92, doi:10.1017/S0967026201003481, 2002.
- 894 Lê, S., Josse, J. and Husson, F.: FactoMineR: an R package for multivariate analysis, Journal of
895 Statistical Software, 25(1), 2008.
- 896 Long, J. D., Smalley, G. W., Barsby, T., Anderson, J. T. and Hay, M. E.: Chemical cues induce
897 consumer-specific defenses in a bloom-forming marine phytoplankton, Proceedings of the
898 National Academy of Sciences, 104(25), 10512–10517 [online] Available from:
899 http://ieeexplore.ieee.org/xpls/abs_all.jsp?arnumber=4224216, 2007.
- 900 Lovenduski, N. S., Gruber, N. and Doney, S. C.: Toward a mechanistic understanding of the
901 decadal trends in the Southern Ocean carbon sink, Global Biogeochemical Cycles, 22(GB3016),
902 doi:10.1029/2007GB003139, 2008.
- 903 Lubbers, G., Gieskes, W., Del Castilho, P., Salomons, W., and Bril, J.: Manganese accumulation
904 in the high pH microenvironment of *Phaeocystis sp.* (Haptophyceae) colonies from the North
905 Sea, Marine Ecology Progress Series, 1990. 285-293, 1990.
- 906 Luxem, K. E., Ellwood, M. J., and Strzepek, R. F.: Intraspecific variability in *Phaeocystis*

- 907 *antarctica*'s response to iron and light stress, PLoS ONE, 12, e0179751, 2017.
- 908 Martin, J. H., Fitzwater, S. E. and Gordon, R. M.: Iron deficiency limits phytoplankton growth in
909 Antarctic waters, Global Biogeochemical Cycles, 4(1), 5–12, doi:10.1029/GB004i001p00005,
910 1990.
- 911 Matrai, P. A., Vernet, M., Hood, R., Jennings, A., Brody, E. and Saemundsdottir, S.: Light-
912 dependence of carbon and sulfur production by polar clones of the genus *Phaeocystis*, Marine
913 Biology, 124, 157–167, 1995.
- 914 Maucher, J. M. and G. R. DiTullio (2003). Flavodoxin as a Diagnostic Indicator of Chronic Fe-
915 Limitation in the Ross Sea and New Zealand Sector of the Southern Ocean. Biogeochemistry in
916 the Ross Sea. G. R. DiTullio and R. B. Dunbar. Washington DC, AGU: 209-220.
- 917 Michel, G., Tonon, T., Scornet, D., Cock, J. M. and Kloareg, B.: The cell wall polysaccharide
918 metabolism of the brown alga *Ectocarpus siliculosus*. Insights into the evolution of extracellular
919 matrix polysaccharides in Eukaryotes, New Phytologist, 188(1), 82–97, 2010.
- 920 Morris, R. M., Nunn, B. L., Frazar, C., Goodlett, D. R., Ting, Y. S. and Rocap, G.: Comparative
921 metaproteomics reveals ocean-scale shifts in microbial nutrient utilization and energy
922 transduction, The ISME Journal, 4(5), 673–685, doi:10.1038/ismej.2010.4, 2010.
- 923 Morrissey, J., Sutak, R., Paz-Yepes, J., Tanaka, A., Moustafa, A., Veluchamy, A., Thomas, Y.,
924 Botebol, H., Bouget, F.-Y., McQuaid, J. B., Tirichine, L., Allen, A. E., Lesuisse, E. and Bowler,
925 C.: A novel protein, ubiquitous in marine phytoplankton, concentrates iron at the cell surface and
926 facilitates uptake, Current Biology, 25, 364–371, doi:10.1016/j.cub.2014.12.004, 2015.
- 927 Murray, A. E. and Grzymalski, J. J.: Diversity and genomics of Antarctic marine micro-organisms,
928 Philosophical Transactions of the Royal Society B: Biological Sciences, 362(1488), 2259–2271,
929 doi:10.1098/rstb.2006.1944, 2007.
- 930 Noble, A. E., Moran, D. M., Allen, A. E. and Saito, M. A.: Dissolved and particulate trace metal
931 micronutrients under the McMurdo Sound seasonal sea ice: basal sea ice communities as a
932 capacitor for iron, Frontiers in Chemistry, 1(25), 1–18, doi:10.3389/fchem.2013.00025, 2013.
- 933 Peers, G. and Price, N. M.: Copper-containing plastocyanin used for electron transport by an
934 oceanic diatom, Nature, 441(7091), 341–344, doi:10.1038/nature04630, 2006.
- 935 Podell, S. and Gaasterland, T.: DarkHorse: a method for genome-wide prediction of horizontal
936 gene transfer, Genome Biology, 8, R16, doi:10.1186/gb-2007-8-2-r16, 2007.
- 937 Ram, R. J., VerBerkmoes, N. C., Thelen, M. P., Tyson, G. W., Baker, B. J., Blake, R. C., Shah,
938 M., Hettich, R. and Banfield, J.: Community proteomics of a natural microbial biofilm, Science,
939 308(5730), 1915–1920, doi:10.1126/science, 2005.
- 940 Rho, M., Tang, H. and Ye, Y.: FragGeneScan: predicting genes in short and error-prone reads,
941 Nucleic Acids Research, 38(20), e191–e191, doi:10.1093/nar/gkq747, 2010.

- 942 Riegman, R. and van Boekel, W.: The ecophysiology of *Phaeocystis globosa*: a review, Journal
943 of Sea Research, 35(4), 235–242, 1996.
- 944 Riegman, R., Noordeloos, A. A. M. and Cadee, G. C.: *Phaeocystis* blooms and eutrophication of
945 the continental coastal zones of the North Sea, Marine Biology, 112, 479–484,
946 doi:10.1007/BF00356293, 1992.
- 947 Roche, J. L., Boyd, P. W., McKay, R. M. L. and Geider, R. J.: Flavodoxin as an *in situ* marker
948 for iron stress in phytoplankton, Nature, 382, 802–805, doi:10.1038/382802a0, 1996.
- 949 Rousseau, V., Chrétiennot-Dinet, M.-J., Jacobsen, A., Verity, P. G. and Whipple, S.: The life
950 cycle of *Phaeocystis*: state of knowledge and presumptive role in ecology, Biogeochemistry, 83,
951 29–47, doi:10.1007/s10533-007-9085-3, 2007.
- 952 Rousseau, V., Mathot, S. and Lancelot, C.: Calculating carbon biomass of *Phaeocystis sp.* from
953 microscopic observations, Marine Biology, 107, 305–314, 1990.
- 954 Saito, M. A., Dorsk, A., Post, A. F., McIlvin, M. R., Rappé, M. S., R, D. G. and Moran, D. M.:
955 Needles in the blue sea: Sub-species specificity in targeted protein biomarker analyses within the
956 vast oceanic microbial metaproteome, Proteomics, 15(20), 3521–3531,
957 doi:10.1002/pmic.201400630, 2015.
- 958 Saito, M. A., Goepfert, T. J., Noble, A. E., Bertrand, E. M., Sedwick, P. N. and DiTullio, G. R.:
959 A seasonal study of dissolved cobalt in the Ross Sea, Antarctica: micronutrient behavior,
960 absence of scavenging, and relationships with Zn, Cd, and P, Biogeosciences, 7, 4059–4082,
961 doi:10.5194/bg-7-4059-2010, 2010.
- 962 Saito, M. A., McIlvin, M. R., Moran, D. M., Goepfert, T. J., R, D. G., Post, A. F. and Lamborg,
963 C. H.: Multiple nutrient stresses at intersecting Pacific Ocean biomes detected by protein
964 biomarkers, Science, 345(6201), 1173–1177, 2014.
- 965 Sarmiento, J. L., Hughes, T. M. C., Stouffer, R. J. and Manabe, S.: Simulated response of the
966 ocean carbon cycle to anthropogenic climate warming, Nature, 393, 245–249,
967 doi:10.1038/30455, 1998.
- 968 Schoemann, V., Becquevort, S., Stefels, J., Rousseau, V. and Lancelot, C.: *Phaeocystis* blooms
969 in the global ocean and their controlling mechanisms: a review, Journal of Sea Research, 53, 43–
970 66, 2005.
- 971 Schoemann, V., Wollast, R., Chou, L. and Lancelot, C.: Effects of photosynthesis on the
972 accumulation of Mn and Fe by *Phaeocystis* colonies, Limnology and Oceanography, 46(5),
973 1065–1076, 2001.
- 974 Sedwick, P. N. and DiTullio, G. R.: Regulation of algal blooms in Antarctic shelf waters by the
975 release of iron from melting sea ice, Geophys. Res. Lett., 24(20), 2515–2518,
976 doi:10.1029/97GL02596, 1997.
- 977 Sedwick, P. N., DiTullio, G. R. and Mackey, D. J.: Iron and manganese in the Ross Sea,

- 978 Antarctica: Seasonal iron limitation in Antarctic shelf waters, *Journal of Geophysical Research*,
979 105(C5), 11321–11336, doi:10.1029/2000JC000256, 2000.
- 980 Sedwick, P. N., Garcia, N. S., Riseman, S. F., Marsay, C. M. and DiTullio, G. R.: Evidence for
981 high iron requirements of colonial *Phaeocystis antarctica* at low irradiance, *Biogeochemistry*,
982 83(1-3), 83–97, doi:10.1007/s10533-007-9081-7, 2007.
- 983 Sedwick, P. N., Marsay, C. M., Sohst, B. M., Aguilar Islas, A. M., Lohan, M. C., Long, M. C.,
984 Arrigo, K. R., Dunbar, R. B., Saito, M. A., Smith, W. O. and DiTullio, G. R.: Early season
985 depletion of dissolved iron in the Ross Sea polynya: Implications for iron dynamics on the
986 Antarctic continental shelf, *Journal of Geophysical Research*, 116(C12019), 2011.
- 987 Smith, W. O., Jr, Codispoti, L. A., Nelson, D. M., Manley, T., Buskey, E. J., Niebauer, H. J. and
988 Cota, G. F.: Importance of *Phaeocystis* blooms in the high-latitude ocean carbon cycle, *Nature*,
989 352, 514–516, 1991.
- 990 Smith, W. O., Jr, Dennett, M. R., Mathot, S. and Caron, D. A.: The temporal dynamics of the
991 flagellated and colonial stages of *Phaeocystis antarctica* in the Ross Sea, *Deep-Sea Research*
992 Part II, 50, 605–617, 2003.
- 993 Smith, W. O., Tozzi, S., Long, M. C., Sedwick, P. N., Peloquin, J. A., Dunbar, R. B., Hutchins,
994 D. A., Kolber, Z. and R, D. G.: Spatial and temporal variations in variable fluorescence in the
995 Ross Sea (Antarctica): Oceanographic correlates and bloom dynamics, *Deep Sea Research I*, 79,
996 141–155, 2013.
- 997 Solomon, C. M., Lessard, E. J., Keil, R. G. and Foy, M. S.: Characterization of extracellular
998 polymers of *Phaeocystis globosa* and *P. antarctica*, *Marine Ecology Progress Series*, 250, 81–
999 89, 2003.
- 1000 Sowell, S. M., Wilhelm, L. J., Norbeck, A. D., Lipton, M. S., Nicora, C. D., Barofsky, D. F., H,
1001 C., Smith, R. D. and Giovanonni, S. J.: Transport functions dominate the SAR11 metaproteome
1002 at low-nutrient extremes in the Sargasso Sea, *The ISME Journal*, 3(1), 93–105,
1003 doi:10.1038/ismej.2008.83, 2008.
- 1004 Stingl, U., Desiderio, R. A., Cho, J. C., Vergin, K. L. and Giovannoni, S. J.: The SAR92 Clade:
1005 an Abundant Coastal Clade of Culturable Marine Bacteria Possessing Proteorhodopsin, *Applied*
1006 *and Environmental Microbiology*, 73(7), 2290–2296, doi:10.1128/AEM.02559-06, 2007.
- 1007 Strzepek, R. F., Maldonado, M. T., Hunter, K. A., Frew, R. D. and Boyd, P. W.: Adaptive
1008 strategies by Southern Ocean phytoplankton to lessen iron limitation: Uptake of organically
1009 complexed iron and reduced cellular iron requirements, *Limnology and Oceanography*, 56(6),
1010 1983–2002, doi:10.4319/lo.2011.56.6.1983, 2011.
- 1011 Sunda, W. and Huntsman, S.: Effect of pH, light, and temperature on Fe–EDTA chelation and Fe
1012 hydrolysis in seawater, *Marine Chemistry*, 84(1-2), 35–47, doi:10.1016/S0304-4203(03)00101-4,
1013 2003.
- 1014 Sunda, W. G. and Huntsman, S. A.: Iron uptake and growth limitation in oceanic and coastal

- 1015 phytoplankton, *Marine Chemistry*, 50, 189–206, 1995.
- 1016 Thingstad, F. and Billen, G.: Microbial degradation of *Phaeocystis* material in the water column,
1017 *Journal of Marine Systems*, 5, 55–65, doi:10.1016/0924-7963(94)90016-7, 1994.
- 1018 Tzarfati-Majar, V., Burstyn-Cohen, T. and Klar, A.: F-spondin is a contact-repellent molecule
1019 for embryonic motor neurons, *Proceedings of the National Academy of Sciences*, 98(8), 4722–
1020 4727, 2011.
- 1021 van Boekel, W.: *Phaeocystis* colony mucus components and the importance of calcium ions for
1022 colony stability, *Marine Ecology Progress Series*, 87, 301–305, 1992.
- 1023 Vardi, A.: Cell signaling in marine diatoms, *Communicative & Integrative Biology*, 1(2), 134–
1024 136, doi:10.1016/j.cub.2008.05.037, 2008.
- 1025 VerBerkmoes, N. C., Hervey, W. J., Shah, M., Land, M., Hauser, L., Larimer, F. W., Van
1026 Berkel, G. J., and Goeringer, D. E.: Evaluation of “shotgun” proteomics for identification of
1027 biological threat agents in complex environmental matrixes: experimental simulations,
1028 *Analytical chemistry*, 77, 923-932, 2005.
- 1029
1030 Verity, P. G., Brussaard, C. P., Nejstgaard, J. C., van Leeuwe, M. A., Lancelot, C. and Medlin,
1031 L. K.: Current understanding of *Phaeocystis* ecology and biogeochemistry, and perspectives for
1032 future research, *Biogeochemistry*, 83, 311–330, doi:10.1007/s10533-007-9090-6, 2007.
- 1033 Warnes, G. R., Bolker, B., Bonebakker, L., Gentleman, R., Huber, W., Liaw, A., Lumley, T.,
1034 Maechler, M., Magnusson, A., Moeller, S. and Schwartz, M.: gplots: Various R programming
1035 tools for plotting data. 2009.
- 1036 Watanabe, Y., Hayashi, M., Yagi, T. and Kamiya, R.: Turnover of actin in *Chlamydomonas*
1037 flagella detected by fluorescence recovery after photobleaching (frap), *Cell*, 29, 67–72,
1038 doi:10.1247/csf.29.67, 2004.
- 1039 Whitney, L. P., Lins, J. J., Hughes, M. P., Wells, M. L., Chappell, P. D. and Jenkins, B. D.:
1040 Characterization of putative iron responsive genes as species-specific indicators of iron stress in
1041 *Thalassiosiroid* diatoms, *Frontiers in Microbiology*, 2, 1–14,
1042 doi:10.3389/fmicb.2011.00234/abstract, 2011.
- 1043 Williams, T. J., Long, E., Evans, F., DeMaere, M. Z., Lauro, F. M., Raftery, M. J., Ducklow, H.,
1044 Grzymalski, J. J., Murray, A. E. and Cavicchioli, R.: A metaproteomic assessment of winter and
1045 summer bacterioplankton from Antarctic Peninsula coastal surface waters, *The ISME Journal*,
1046 6(10), 1883–1900, doi:10.1038/ismej.2012.28, 2012.
- 1047 Wu, Z., Jenkins, B. D., Rynearson, T. A., Dyhrman, S. T., Saito, M. A., Mercier, M. and
1048 Whitney, L. P.: Empirical bayes analysis of sequencing-based transcriptional profiling without
1049 replicates, *BMC Bioinformatics*, 11, 564, doi:10.1186/1471-2105-11-564, 2010.
- 1050 Zilliges, Y., Kehr, J. C., Mikkat, S., Bouchier, C., de Marsac, N. T., Borner, T. and Dittmann, E.:
1051 An extracellular glycoprotein is implicated in cell-cell contacts in the toxic cyanobacterium

- 1052 *Microcystis aeruginosa* PCC 7806, Journal of Bacteriology, 190(8), 2871–2879,
1053 doi:10.1128/JB.01867-07, 2008.
- 1054 Zingone, A., Chrétiennot-Dinet, M.-J., Lange, M. and Medlin, L.: Morphological and genetic
1055 characterization of *Phaeocystis cordata* and *P. jahnii* (prymnesiophyceae), two new species from
1056 the Mediterranean Sea, Journal of Phycology, 35(6), 1322–1337, doi:10.1046/j.1529-
1057 8817.1999.3561322.x, 1999.
- 1058 Zurbriggen, M. D., Tognetti, V. B., Fillat, M. F., Hajirezaei, M.-R., Valle, E. M. and Carrillo, N.:
1059 Combating stress with flavodoxin: a promising route for crop improvement, Trends in
1060 Biotechnology, 26(10), 531–537, 2008.
- 1061